CHAPTER 6

ELECTROCHEMICAL IMPEDANCE STUDIES

6.1 Introduction

The objective of this chapter is to determine the conductivity of the samples at room and elevated temperatures and also to study the dielectric properties and obtain the transport parameters. In this chapter, results on the studies of two electrolyte systems PVA-chitosan-NH_4NO_3 and PVA-chitosan-NH_4NO_3-EC will be presented. The polymer host is a blend of chitosan and PVA in the ratio 2:3. This blend is the most amorphous and homogeneous. NH_4NO_3 was added to the blended polymer solution and the highest conducting polymer-salt sample was plasticized with ethylene carbonate (EC) to obtain the maximum conductivity enhanced sample. The Rice and Roth model [Rice and Roth, 1972] was employed to estimate the number density of ions per cm^3 with the hope to gain some understanding on the variation of conductivity with the doping salt content.

6.2 Conductivity Studies for Salted System

Figure 6.1 represents one of the Cole-Cole plots for the pure PVA-chitosan blended film (C4P6) at room temperature after storage in a dessicant filled dessicator for 15 days. The purpose of plotting the Zi versus Zr or Cole-Cole plot is to determine the bulk resistance value that will be used in the calculation of the sample conductivity.

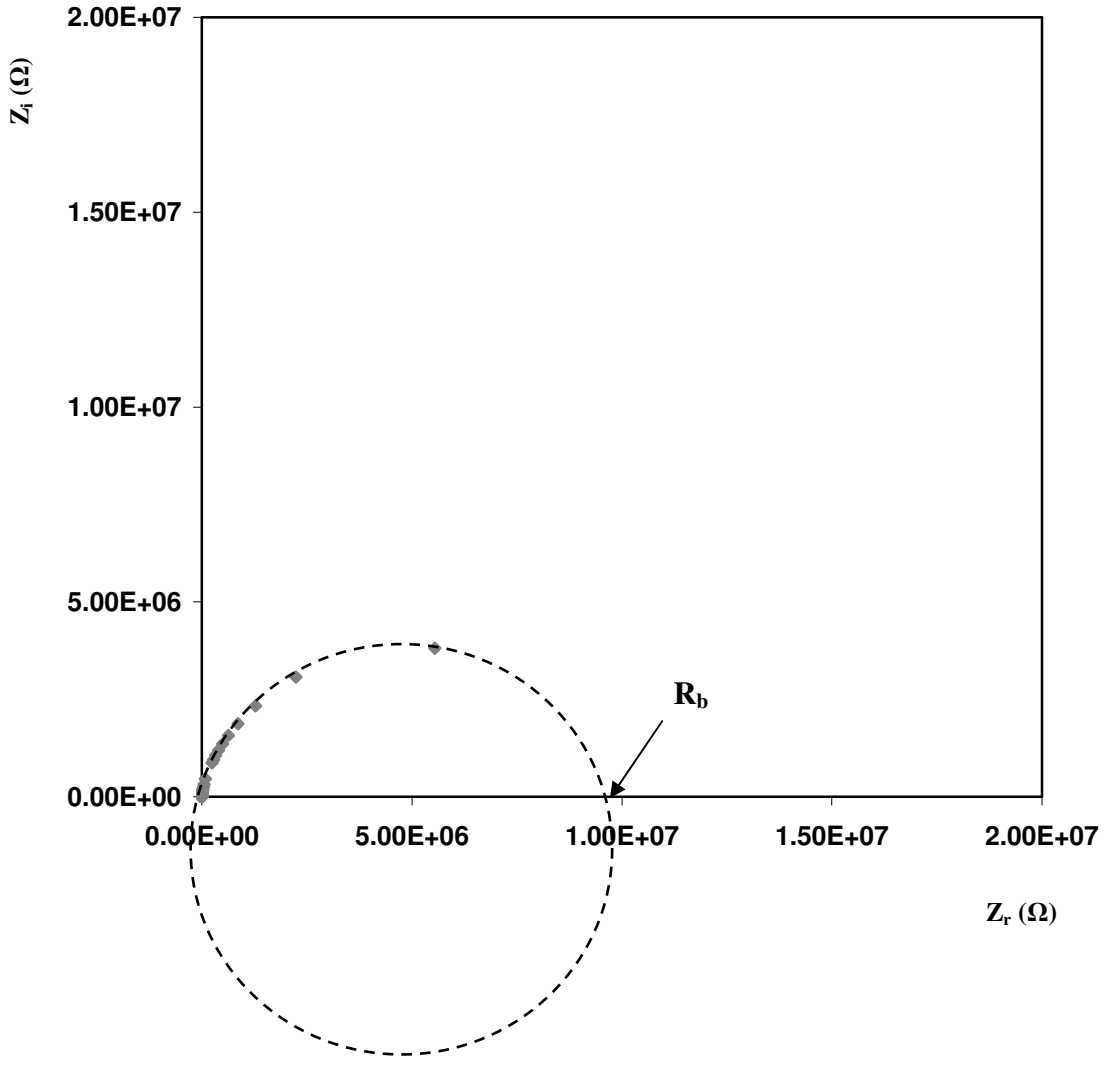

Figure 6.1: Cole-Cole plot of the pure C4P6 film.

The Cole-Cole plot of the C4P6 membrane shows a tilted semicircle implying that the material is partially resistive and capacitive.

Figure 6.2 represents the Cole-Cole plot of the highest conducting sample in the salted system for the sample 60[C4P6]-40AN. The salt added to the sample provides a charged species for the polymer to conduct, and for the present study the charge species is H^+. It can be observed that after the addition of salt, the polymer electrolyte has become very capacitive in nature. The capacitance of these doped samples changes with frequency.

The addition of salt in the plasticizer free system was stopped until 60 wt.% of NH_4NO_3 since on addition of more than 60 wt.% salt, the film is difficult to peel, brittle and low in mechanical strength.

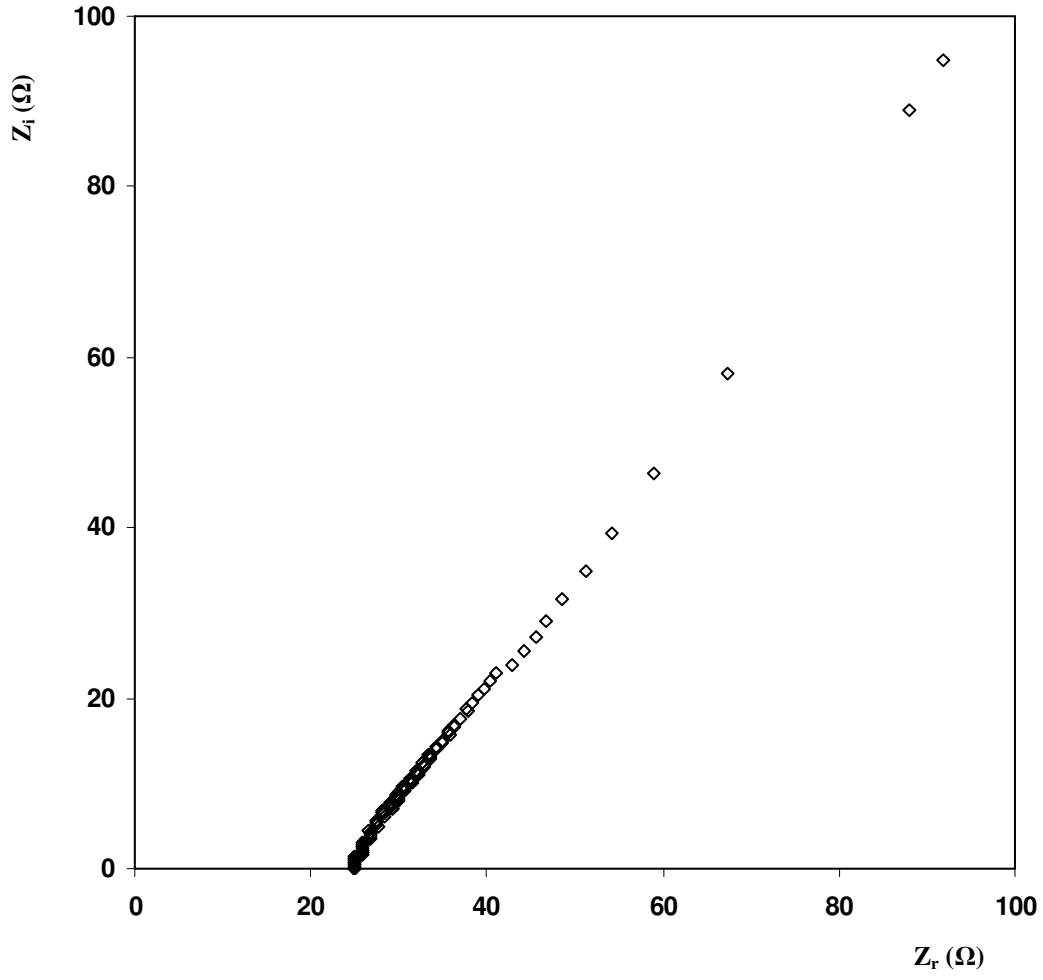

Figure 6.2: Cole-Cole plot of the sample film 60[C4P6]-40AN.

From Figure 6.3, it is shown that the conductivity of pure PVA-chitosan polymer blend film is low, about 4.48 x 10^{-11} S cm^{-1} at room temperature. The ionic conductivity is observed to increase gradually until 2.07 x 10^{-5} S cm^{-1} when 40 wt.% NH_4NO_3 was added. Beyond the amount of 40 wt.% NH_4NO_3 salt, the conductivity decreases.

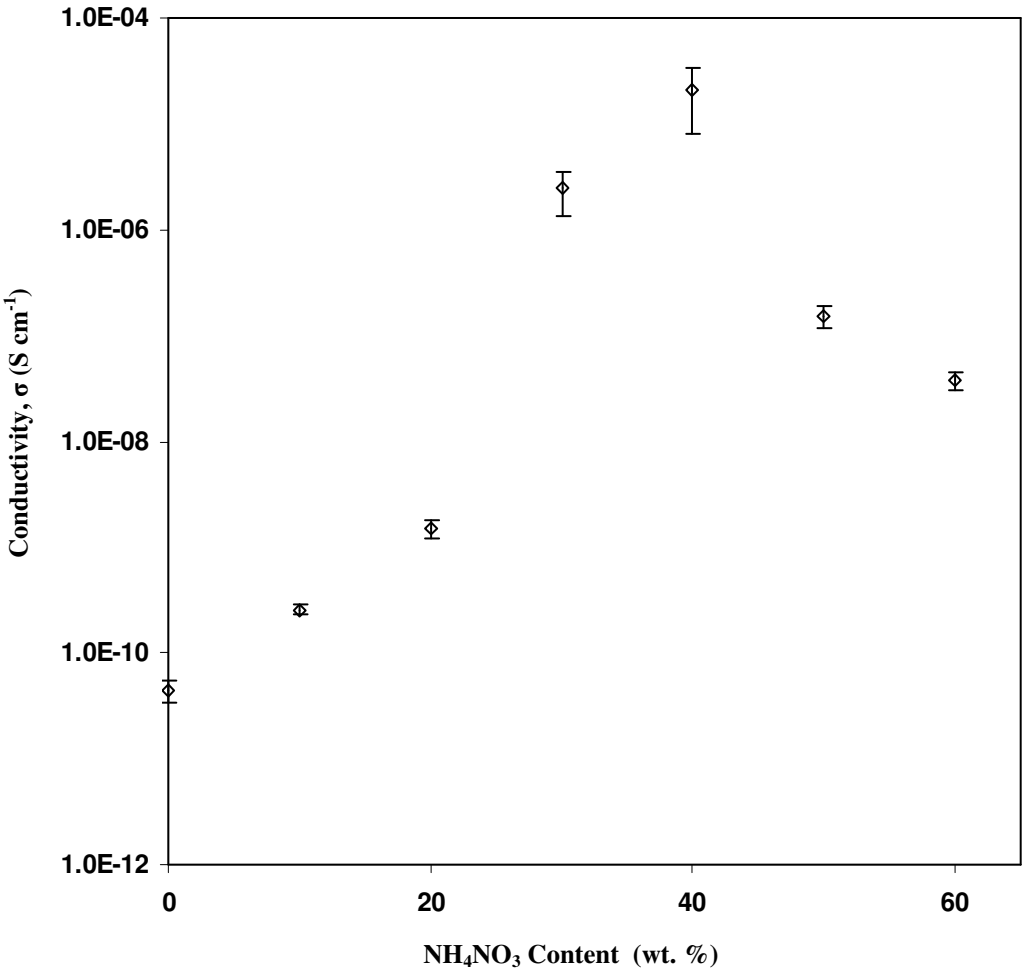

Figure 6.3: The dependence of ionic conductivity of salted system at room temperature.

With increase in salt concentration from 10 to 40 wt.% NH_4NO_3, the conductivity increase is attributable to the increase in number density of mobile ions provided by the increase in salt content. The number density of mobile ions is governed by the rate of ion association and dissociation. Obviously in this concentration range, the rate of ion dissociation has to be greater than the rate of ion association. At higher salt concentrations (above 40 wt.%), the closeness of the dissociated ions may lead to

cation-anion recombination to form neutral ion-pairs that do not contribute towards conductivity [Majid and Arof, 2008]. This results in the lowering of the number density of mobile ions and consequently the conductivity of the samples. Chagnes *et al.,* (2003) added that the high salt concentration can also reduce ionic mobility since this will increase the viscosity of the solution prior to film formation. Besides that the conductivity can decrease due to the formation of neutral salt aggregates that will lessen the numbers of mobile ions. The aggregates can also serve as a hindrance that can slow down the ion travel from one site to another.

In order to see the increase and decrease in conductivity, XRD diffractogram and SEM micrographs can shed some light. Figure 6.4 (a) represents the X-ray diffractogram for the sample film of 60[C4P6]-40AN surface and (b) pure salt of NH_4NO_3.

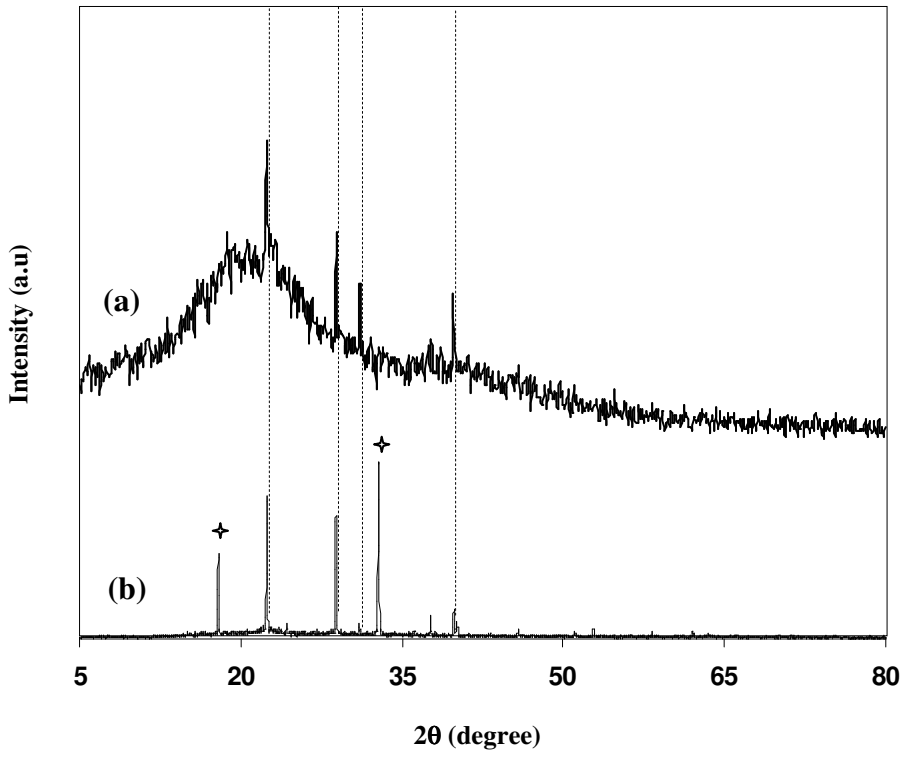

Figure 6.4: XRD diffractogram of (a) 60[C4P6]-40AN film and (b) pure NH_4NO_3.

From Figure 6.4 (a), the diffractogram of the sample surface of 60[C4P6]-40AN shows peaks that can be assigned to NH_4NO_3. The pure NH_4NO_3 salt has a lot of sharp peaks where some of it is situated at 2θ = 17.9º, 22.4º, 28.9º, 31.1º, 32.8º, 37.7º and 39.8º. The peaks that has been observed for the sample of 60[C4P6]-40AN can be attributed to NH_4NO_3 since the peaks are situated at 2θ = 22.4º, 28.9º, 31.1º and 39.8º. However the two sharp peaks at 2θ = 17.9º and 32.8º of pure NH_4NO_3 salt do not appear in the 60[C4P6]-40AN sample.

A large modification on morphology of pure PVA-chitosan blend film can be observed on addition of 40 wt.% NH_4NO_3, Figure 6.5. The surface morphology consists of dispersed grains. These grains are thought to be NH_4^+ ions that have recombined with NO_3^- and trapped under thin layer of the blended film. This is because the X-ray diffractogram in Figure 6.4 (a) shows peaks that can be assigned to ammonium nitrate.

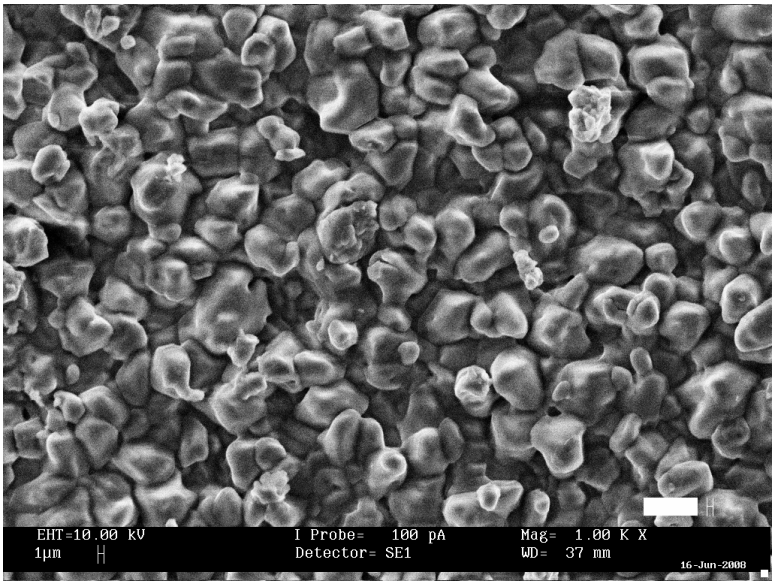

Figure 6.5: SEM surface morphology of 60[C4P6]-40AN film.

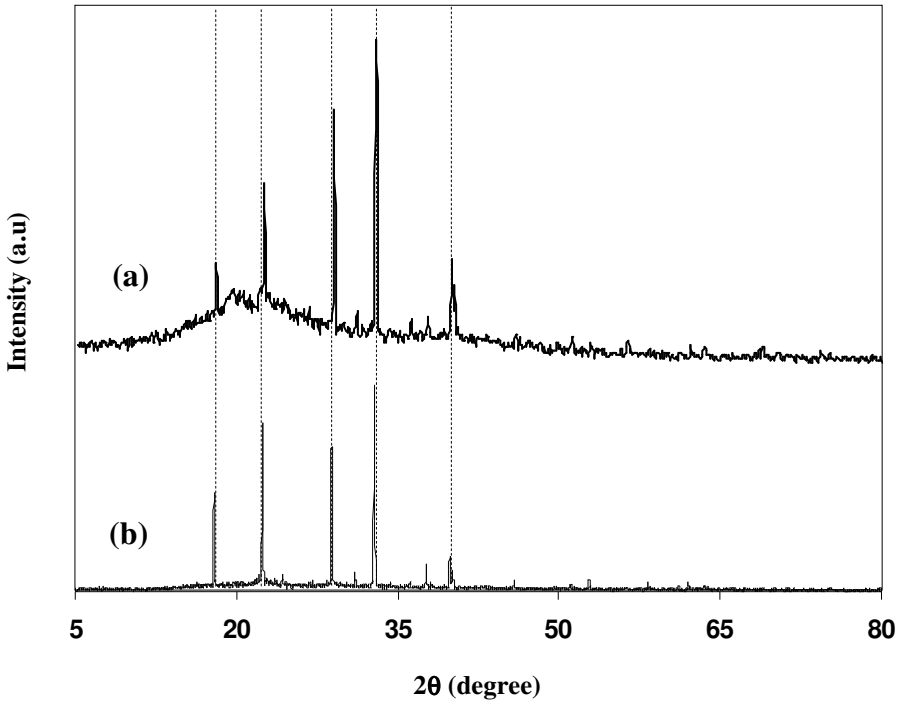

Figure 6.6: XRD diffractogram of (a) 50[C4P6]-50AN film and (b) pure NH_4NO_3.

Figure 6.6 (a) and (b) represents the X-ray diffractogram for the sample film of 50[C4P6]-50AN and pure salt NH_4NO_3 respectively. Five sharp peaks has been observed in sample film of 50[C4P6]-50AN at 2θ = 17.9º, 22.4º, 28.9º, 32.8º and 39.8º that are attributed to the salt. From the XRD pattern it can be concluded that the salt has therefore recrystallized out of the film since conductivity of the system has started to decrease when 50 wt. % NH_4NO_3 was added as depicted in Figure 6.3.

Figure 6.7 represents the SEM micrograph of the sample 50[C4P6]-50AN film surface. The surface exhibits some crystalline features. These crystalline features could be identified as the excess salt or NH_4NO_3 aggregates that have protruded the surface of the polymer electrolytes. This is because the X-ray diffractogram in Figure 6.6 consists of NH_4NO_3 peaks and other additional peaks overlapping with the diffractogram of the polymer host.

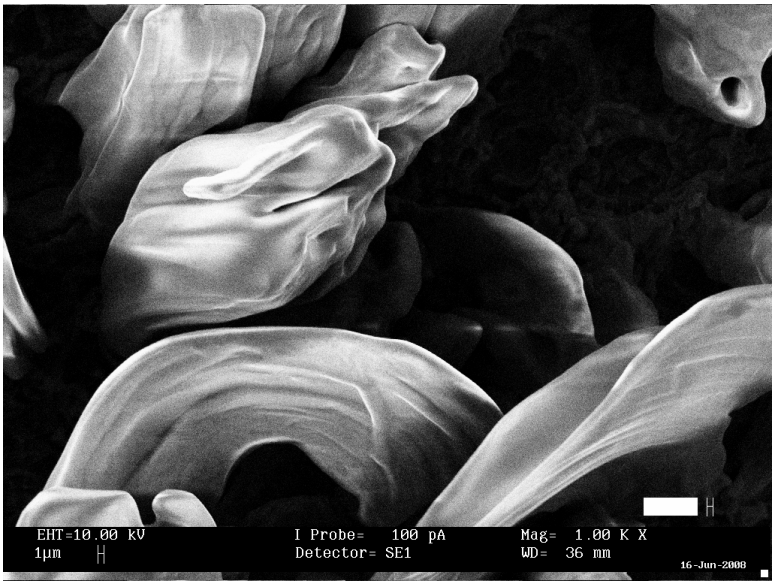

Figure 6.7: SEM surface morphology of 50[C4P6]-50AN film.

As further proof that the conductivity depends on number density of mobile ions, we refer to Figure 6.8 (a) and (b) representing the X-ray diffractograms for the sample 40[C4P6]-60AN and pure salt NH_4NO_3.

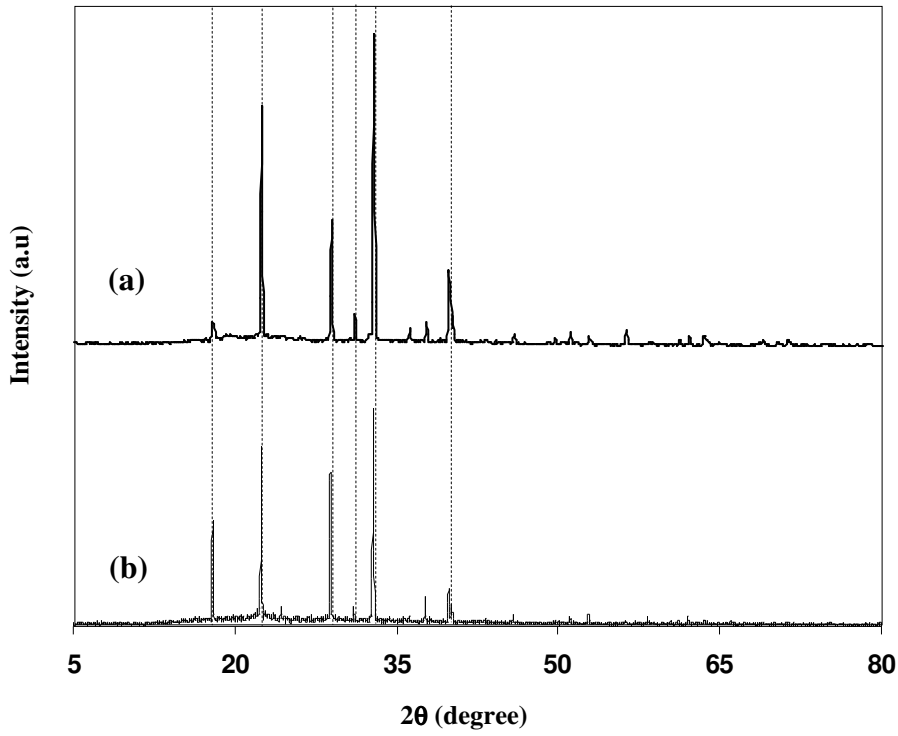

Figure 6.8: XRD diffractogram of (a) 40[C4P6]-60AN film and (b) pure NH_4NO_3.

Peaks observed in the diffractogram of 40[C4P6]-60AN are situated at 2θ = 17.9º, 22.4º, 28.9º, 31.1º, 32.8º and 39.8º. This indicates that the sample of 40[C4P6]-60AN has become more crystalline that leads towards further decrease in conductivity value. It can be observed from the diffractogram that the intensity due to the polymer blend has decreased tremendously compared to intensity of the polymer blend in the diffractogram of 60[C4P6]-40AN.

Figure 6.9: SEM surface morphology of 40[C4P6]-60AN film.

Figure 6.9 shows the SEM micrograph for the surface of the film 40[C4P6]-60AN. When 60 wt. % NH_4NO_3 was added, the morphology consists of solid structures that have protruded the surface of the film. The X-ray diffractogram of the film surface in Figure 6.8 has confirmed that this solid structure in Figure 6.9 is attributed to NH_4NO_3 and its aggregates.

Table 6.1: The average ionic conductivity for salted system at room temperature.

Designation	σ (S cm^{-1})
C4P6	4.48×10^{-11}
90[C4P6]-10AN	2.57×10^{-10}
80[C4P6]-20AN	1.48×10^{-9}
70[C4P6]-30AN	2.42×10^{-6}
60[C4P6]-40AN	2.07×10^{-5}
50[C4P6]-50AN	1.52×10^{-7}
40[C4P6]-60AN	3.74×10^{-8}

6.3 Dielectric Constant Analysis

6.3.1 Dielectric Constant for Salted System at Room Temperature

The dielectric constant indicates the amount of charge that can be stored [Khiar *et al.,* 2006] by a material and it can be used as an indicator to prove that the increase in conductivity is due to an increase in the charge carriers or number of free mobile ions. If the dielectric constant of the material increases, the amount of charge stored by the material will also increase.

The variation of dielectric constant at room temperature of salted system is presented in Figure 6.10. In the frequency range studied no relaxation peaks are observed. The sharp rise in dielectric constant at low frequencies is indicative of space charge effects and electrode polarization confirming that the ions have different relaxation times [Govindaraj *et al.,* 1995; Qian *et al.,* 2001]. From Figure 6.10, it can be observed at a fixed frequency the variation in dielectric constant follows the same trend as the variation in conductivity.

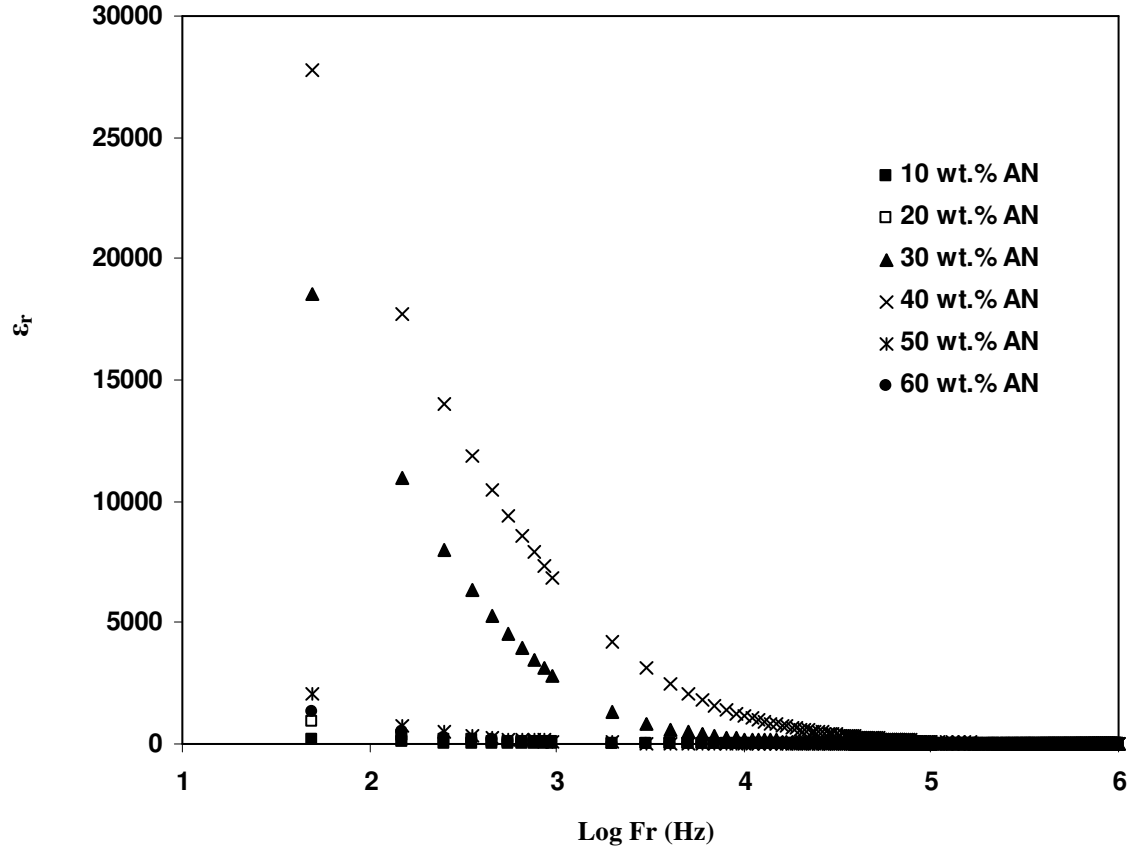

Figure 6.10: Dielectric constant versus frequency for salted system at room temperature.

Table 6.1 shows that the conductivities of salted system at different NH_4NO_3 concentrations, σ (60[C4P6]-40AN) > σ (70[C4P6]-30AN) > σ (50[C4P6]-50AN) > σ (40[C4P6]-60AN) > σ (80[C4P6]-20AN) > σ (90[C4P6]-10AN). The conductivity value in the system is in a good agreement with ε_r where it can be seen in Figure 6.10 that the ε_r (60[C4P6]-40AN) > ε_r (70[C4P6]-30AN) > ε_r (50[C4P6]-50AN) > ε_r (40[C4P6]-60AN) > ε_r (80[C4P6]-20AN) > ε_r (90[C4P6]-10AN). Therefore it can be concluded that the variation in the number of available free mobile ions has influenced the variation in conductivity. Dutta *et al.,* (2002) have supported the conclusion in this study.

6.3.2 Dielectric Constant of Film Sample 60[C4P6]-40AN at Elevated Temperatures

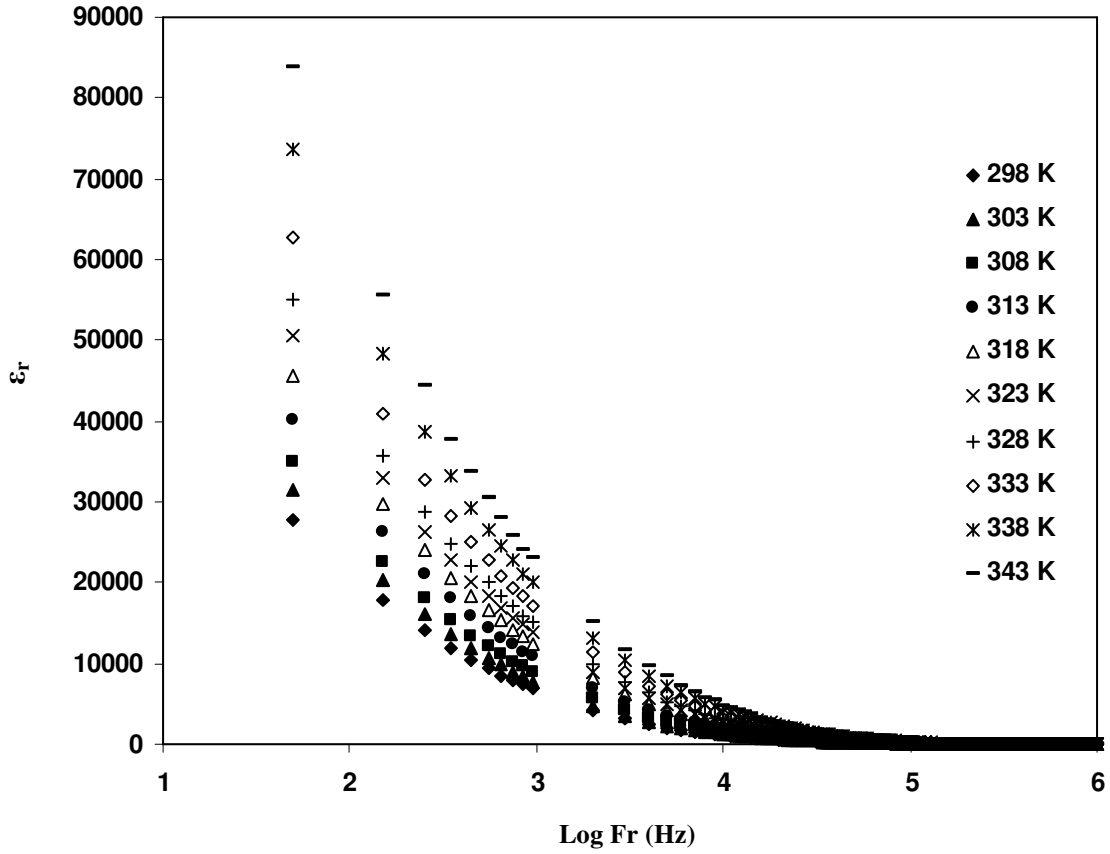

Figure 6.11: Dielectric constant versus frequency for sample 60[C4P6]-40AN at elevated temperatures.

In order to see the effect of temperature on the dielectric analysis, the dielectric data was calculated at room and elevated temperatures until 343 K. The variation of the dielectric constant for the highest conducting sample 60[C4P6]-40AN as a function of frequency at elevated temperatures are as depicted in Figure 6.11. At higher temperatures, the value of dielectric constant is higher. This implies that the increase in conductivity is temperature assisted as temperature increases the neutral ion aggregates may have dissociated due to the vigorous vibrations from the thermal energy supplied on heating. As a result, singlet and triplet ions that can contribute to conductivity enhancement may have formed. Additional mobile ions can also result from

undissociated salt molecules. All this leads to conductivity enhancement. The increase in the number of conductivity contributing ions is reflected in the increase of dielectric constant.

6.4 Temperature Dependence of Conductivity (Salted System)

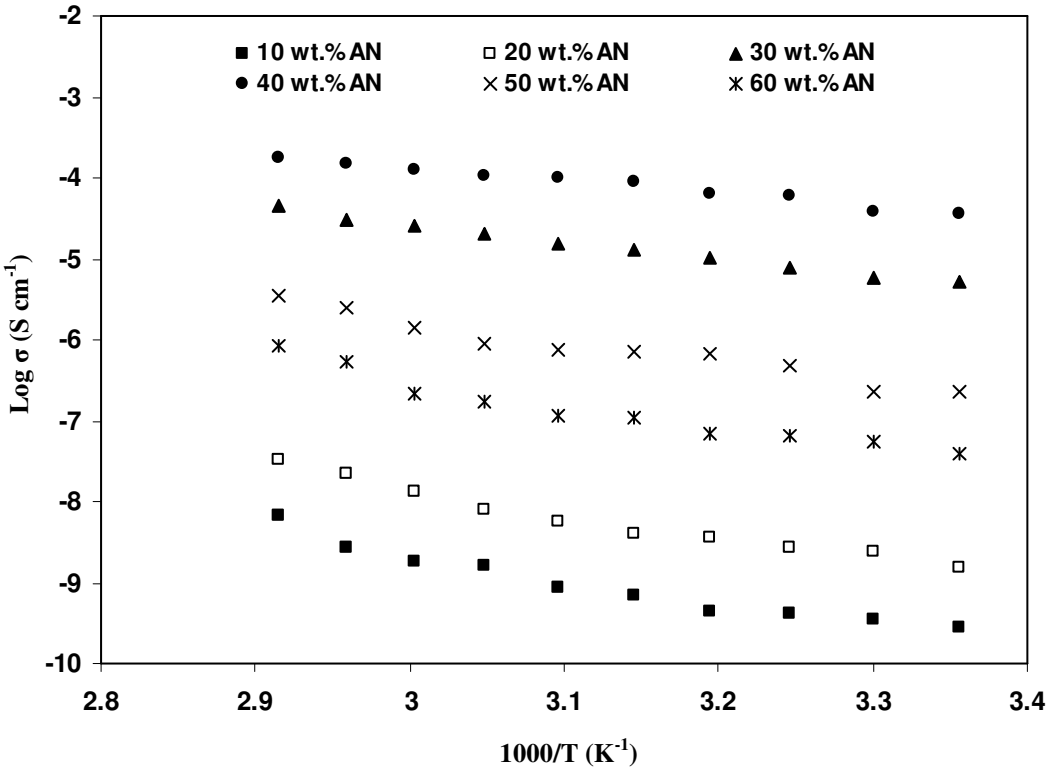

Figure 6.12: Temperature dependent conductivity for salted system.

The change in conductivity of the electrolytes of the salted system from 298 to 343 K is shown in Figure 6.12. The conductivity noticeably increases with temperature. The regression value, R^2 for every line is close to unity and is shown in Table 6.2. The R^2 value lies in the range of 0.92-0.99 indicating that σ-T relationship is Arrhenian and the activation energy can be calculated from the Equation (2.2),

$$\sigma = \sigma_o \exp\left[\frac{-E_a}{kT}\right]$$

Here σ_o the pre exponential factor, E_a is the activation energy, k is the Boltzmann constant and T is the temperature. The Arrhenian conductivity-temperature relationship has been observed for the systems PVA-NH_4Cl, PVA-NH_4Br and PVA-NH_4I [Hema *et al.,* 2008, 2009a, 2009b].

The highest conducting sample (60[C4P6]-40AN) in the salted system possessed the lowest activation energy of 0.30 eV. Figure 6.13 represents the activation energy and conductivity plot of the salted system. From the plot, it can be inferred that E_a (60[C4P6]-40AN) < E_a (70[C4P6]-30AN) < E_a (50[C4P6]-50AN) < E_a (40[C4P6]-60AN) < E_a (80[C4P6]-20AN) < E_a (90[C4P6]-10AN). Figure 6.13 represents the activation energy and the conductivity for the system of C4P6-NH_4NO_3 which has been calculated from the slope of the log σ versus 1000/T. The value of activation energy is listed in Table 6.2.

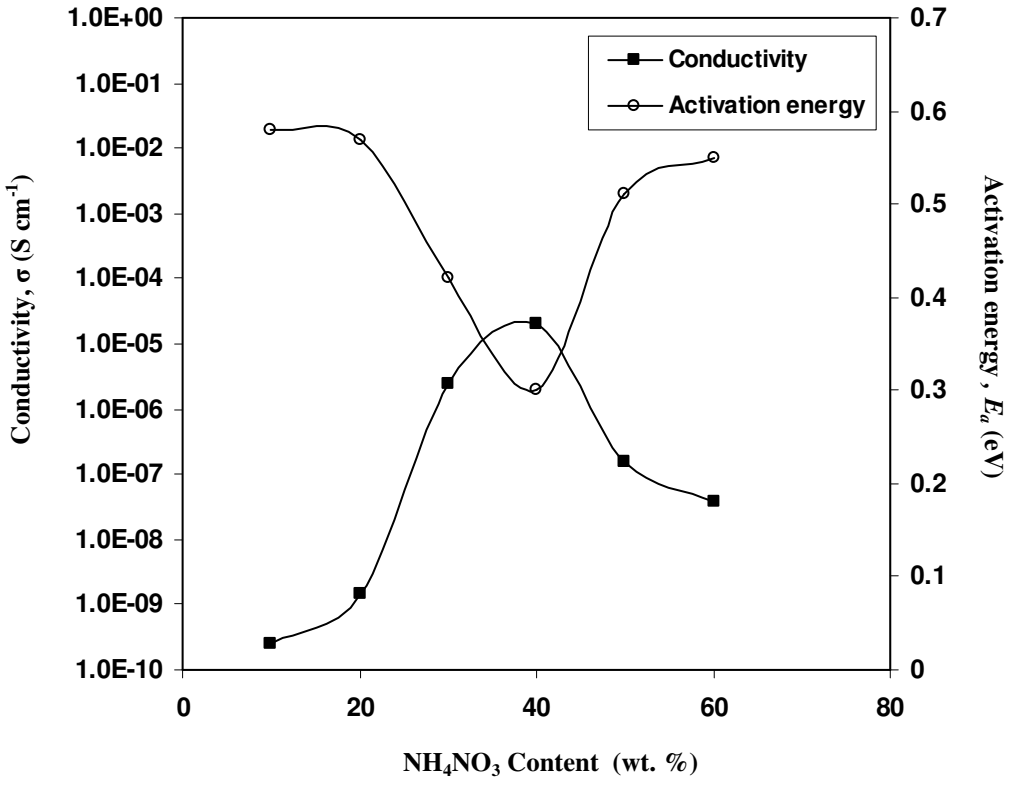

Figure 6.13: Activation energy for salted system.

Table 6.2: Regression, R^2 and activation energy, E_a value for salted system.

Designation	R^2	E_a (eV)
90[C4P6]-10AN	0.93	0.58
80[C4P6]-20AN	0.95	0.57
70[C4P6]-30AN	0.92	0.42
60[C4P6]-40AN	0.98	0.30
50[C4P6]-50AN	0.99	0.51
40[C4P6]-60AN	0.98	0.55

6.5 The Rice and Roth Model for the Salted System

To calculate the number density, mobility and diffusion coefficient of the charge carriers, the Rice and Roth (1972) model was employed to the conductivity data. All the transport parameters data are tabulated in Tables 6.3, 6.4 and 6.5. From Table 6.3, it can be observed that the charge carrier number density increases with conductivity. The highest conducting sample in the salted system has the highest number density of mobile ions of 6.57 x 10^{19} cm^{-3}. The number density of mobile ions decreases for salt content with more than 40 wt.% salt concentration leading to a drop in conductivity. These calculations are in agreement with the results shown in Figure 6.3. From Table 6.3, it can be inferred that NH_4NO_3 in the polymer-salt electrolytes is only partially dissociated into ions. In the salted system the mobility increases from 3.27 x 10^{-7} to 1.97 x 10^{-6} $cm^2 V^{-1} s^{-1}$, as the salt concentration increases from 10 – 40 wt.%. Above 40 wt.% the salt increases the viscosity that the mobility of the ions decreases and the ions require higher activation energy for transport.

Table 6.3: Transport parameters for salted system at room temperature (using l = 10 Å).

Designation	τ (s)	n (cm^{-3})	μ ($cm^2 V^{-1} s^{-1}$)
90[C4P6]-10AN	9.46×10^{-14}	4.91×10^{15}	3.27×10^{-7}
80[C4P6]-20AN	9.54×10^{-14}	2.65×10^{16}	3.49×10^{-7}
70[C4P6]-30AN	1.11×10^{-13}	1.61×10^{19}	9.37×10^{-7}
60[C4P6]-40AN	1.32×10^{-13}	6.57×10^{19}	1.97×10^{-6}
50[C4P6]-50AN	1.01×10^{-13}	1.83×10^{18}	5.21×10^{-7}
40[C4P6]-60AN	9.71×10^{-14}	5.86×10^{17}	3.99×10^{-7}

In this work, various l values were used to calculate the transport parameters. The purpose of using various value of l is because the electrolyte consists of PVA and chitosan blend. It is well known that in chitosan the distance (l) between amine and amine complexed site is 10 Å as reported by Okuyama *et al.,* (2000). In PVA the length between OH and OH is possible in the range of 3 to 6 Å since it is known that the length between carbon and carbon is 1.54 Å. Table 6.4 represents the transport parameters using l = 6 Å. It can be observed that the number density of mobile ions follows the trend of conductivity of the salted systems and for the highest conducting film the number density of mobile ions is 1.10×10^{20} cm^{-3}. The mobility increases from 1.96×10^{-7} to 1.18×10^{-6} $cm^2 V^{-1}s^{-1}$ as the salt content increases from 10 to 40 wt.%. As for the transport parameters using l = 3 Å, it can be seen that the trend of number density of mobile ions follows the trend of conductivity as plotted in Figure 6.3.

Table 6.4: Transport parameters for salted system at room temperature (using l = 6 Å).

Designation	τ (s)	n (cm^{-3})	μ ($cm^2 V^{-1} s^{-1}$)
90[C4P6]-10AN	5.68×10^{-14}	8.18×10^{15}	1.96×10^{-7}
80[C4P6]-20AN	5.73×10^{-14}	4.42×10^{16}	2.10×10^{-7}
70[C4P6]-30AN	6.67×10^{-14}	2.69×10^{19}	5.62×10^{-7}
60[C4P6]-40AN	7.89×10^{-14}	1.10×10^{20}	1.18×10^{-6}
50[C4P6]-50AN	6.05×10^{-14}	3.04×10^{18}	3.13×10^{-7}
40[C4P6]-60AN	5.83×10^{-14}	9.77×10^{17}	2.39×10^{-7}

Table 6.5: Transport parameters for salted system at room temperature (using l = 3 Å).

Designation	τ (s)	n (cm^{-3})	μ ($cm^2 V^{-1} s^{-1}$)
90[C4P6]-10AN	2.84×10^{-14}	1.64×10^{16}	9.80×10^{-8}
80[C4P6]-20AN	2.86×10^{-14}	8.84×10^{16}	1.05×10^{-7}
70[C4P6]-30AN	3.34×10^{-14}	5.37×10^{19}	2.81×10^{-7}
60[C4P6]-40AN	3.95×10^{-14}	2.19×10^{20}	5.91×10^{-7}
50[C4P6]-50AN	3.03×10^{-14}	6.09×10^{18}	1.56×10^{-7}
40[C4P6]-60AN	2.91×10^{-14}	1.95×10^{18}	1.20×10^{-7}

Figures 6.14 and 6.15 represents the variation of number density, n and mobility, μ of ions as functions of temperature respectively. It is clearly observed that the number density of mobile ions increases as the temperature increases as depicted in Figure 6.14. The mobility of ions also increases as the temperature increases however the increment is not so obvious as compared to the number density of ions. Figures 6.16, 6.17, 6.18 and 6.19 represents the variation of number density and mobility as functions of temperature using l = 6 Å and 3 Å respectively and the trend is the same as l = 10 Å.

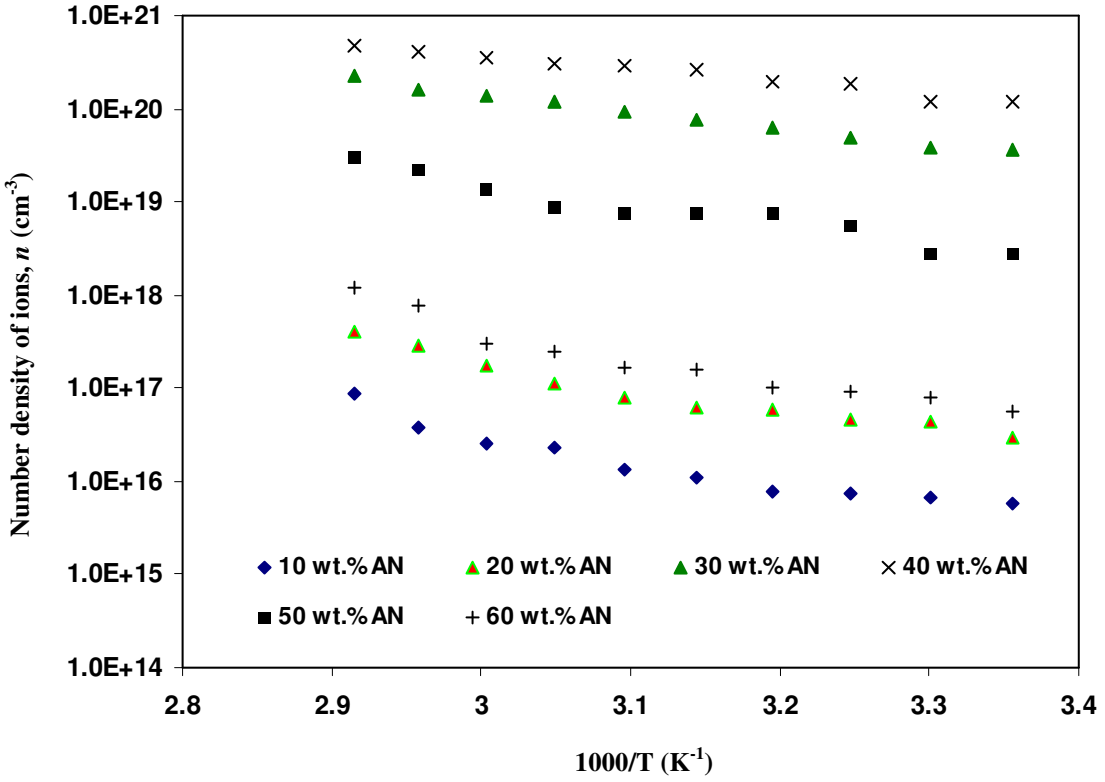

Figure 6.14: Number density of mobile ions, *n* for salted system at different temperatures for *l* = 10 Å.

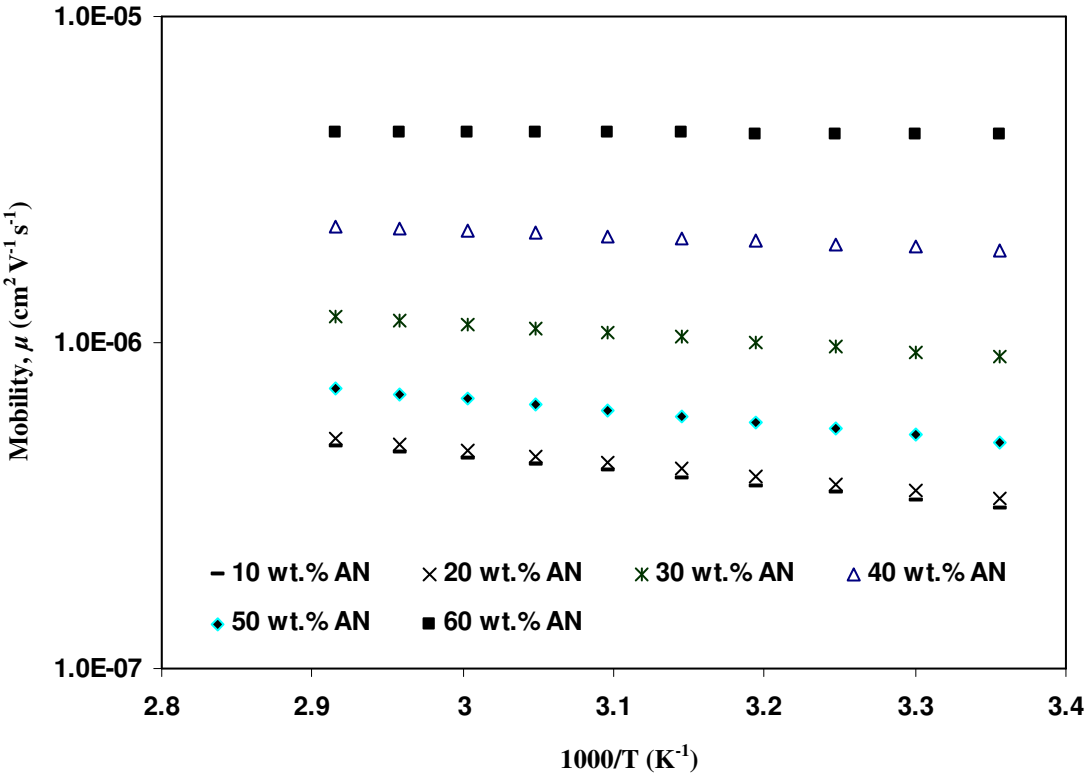

Figure 6.15: Mobility of ions, *μ* for salted system at different temperatures for *l* = 10 Å.

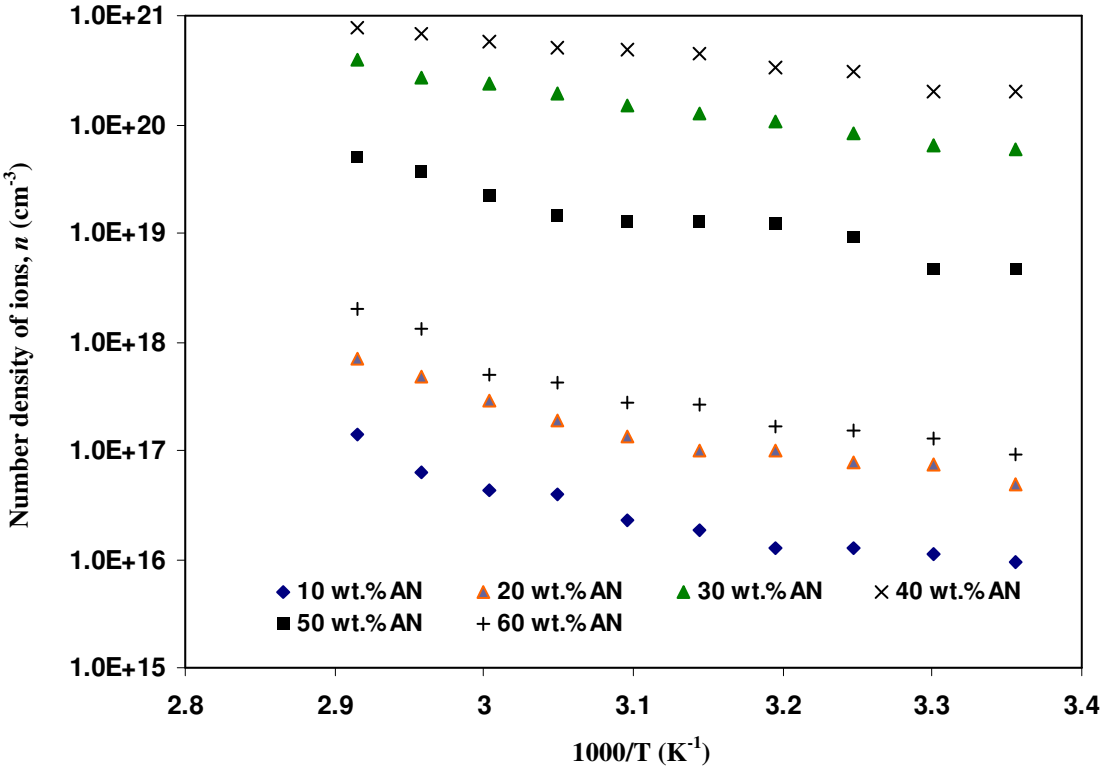

Figure 6.16: Number density of mobile ions, *n* for salted system at different temperatures for *l* = 6 Å.

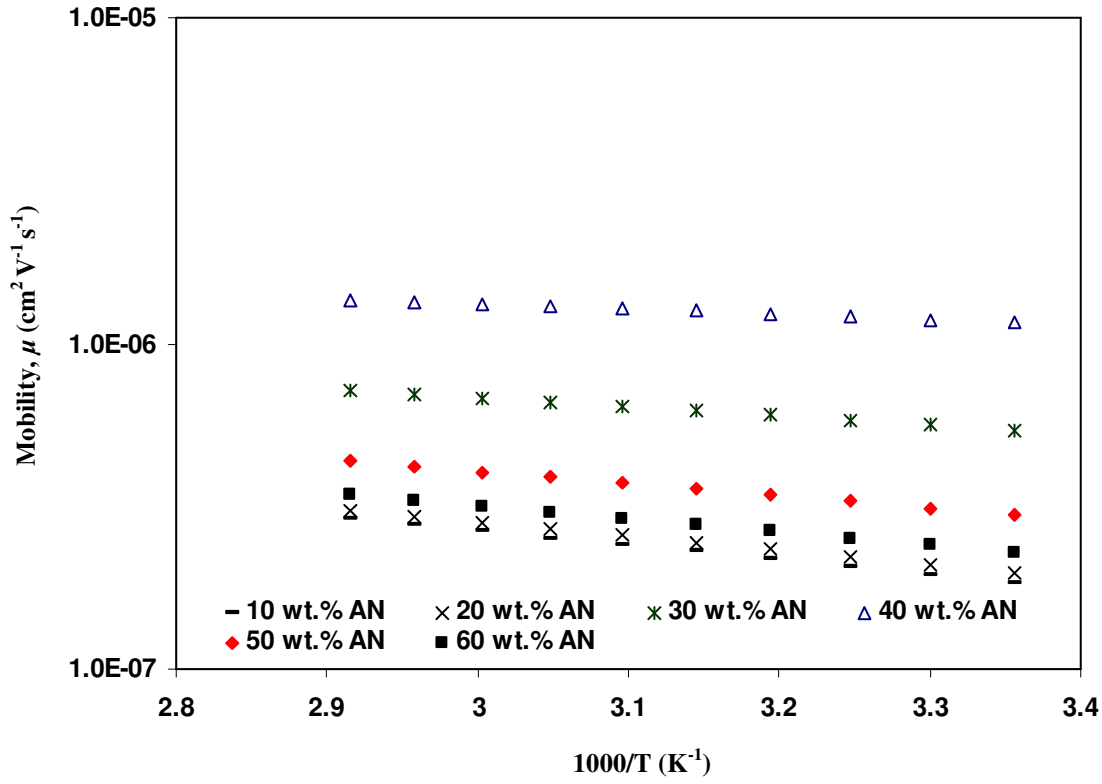

Figure 6.17: Mobility of ions, *μ* for salted system at different temperatures for *l* = 6 Å.

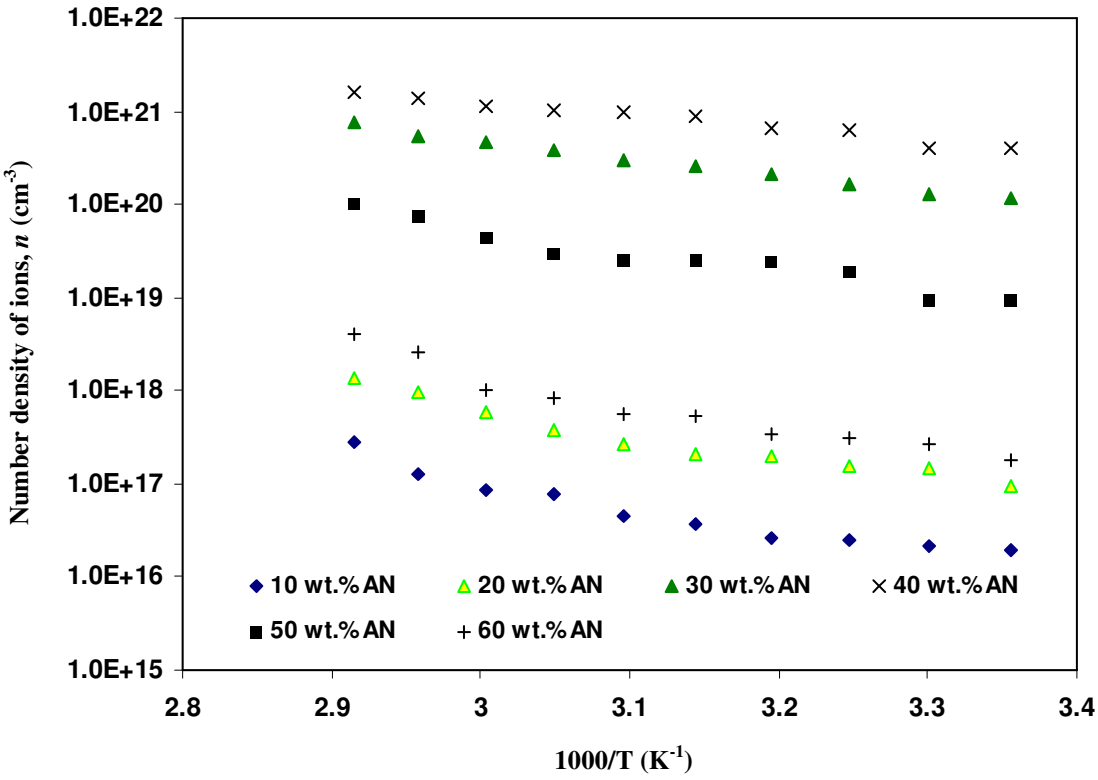

Figure 6.18: Number density of mobile ions, *n* for salted system at different temperatures for *l* = 3 Å.

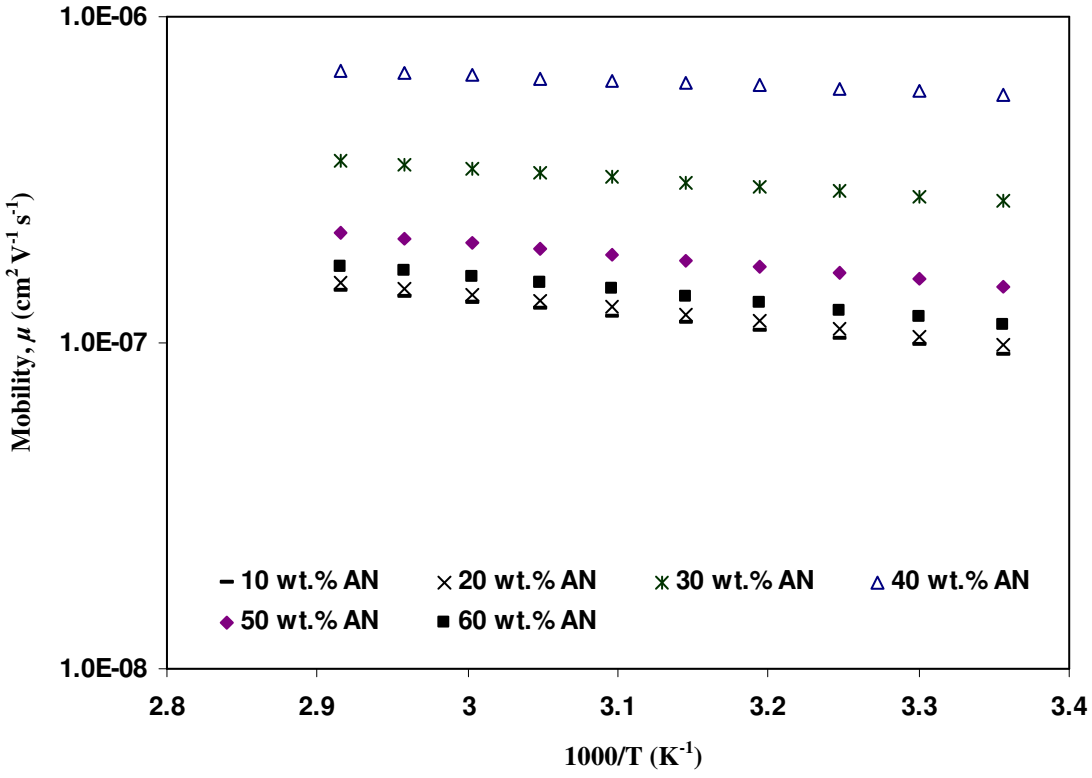

Figure 6.19: Mobility of ions, *μ* for salted system at different temperatures for *l* = 3 Å.

6.6 Conductivity Studies for Plasticized System

Figure 6.20 represents the Cole-Cole plot for the 30[60C4P6-40AN]-70EC film. The Cole-Cole plot of the membrane shows a spike at low frequency region implying that the material is capacitive and the capacitance is frequency dependent.The low frequency spike is attributed to the effect of blocking electrodes [Selvasekarapandian *et al.,* 2005b; Kim *et al.,* 1999].

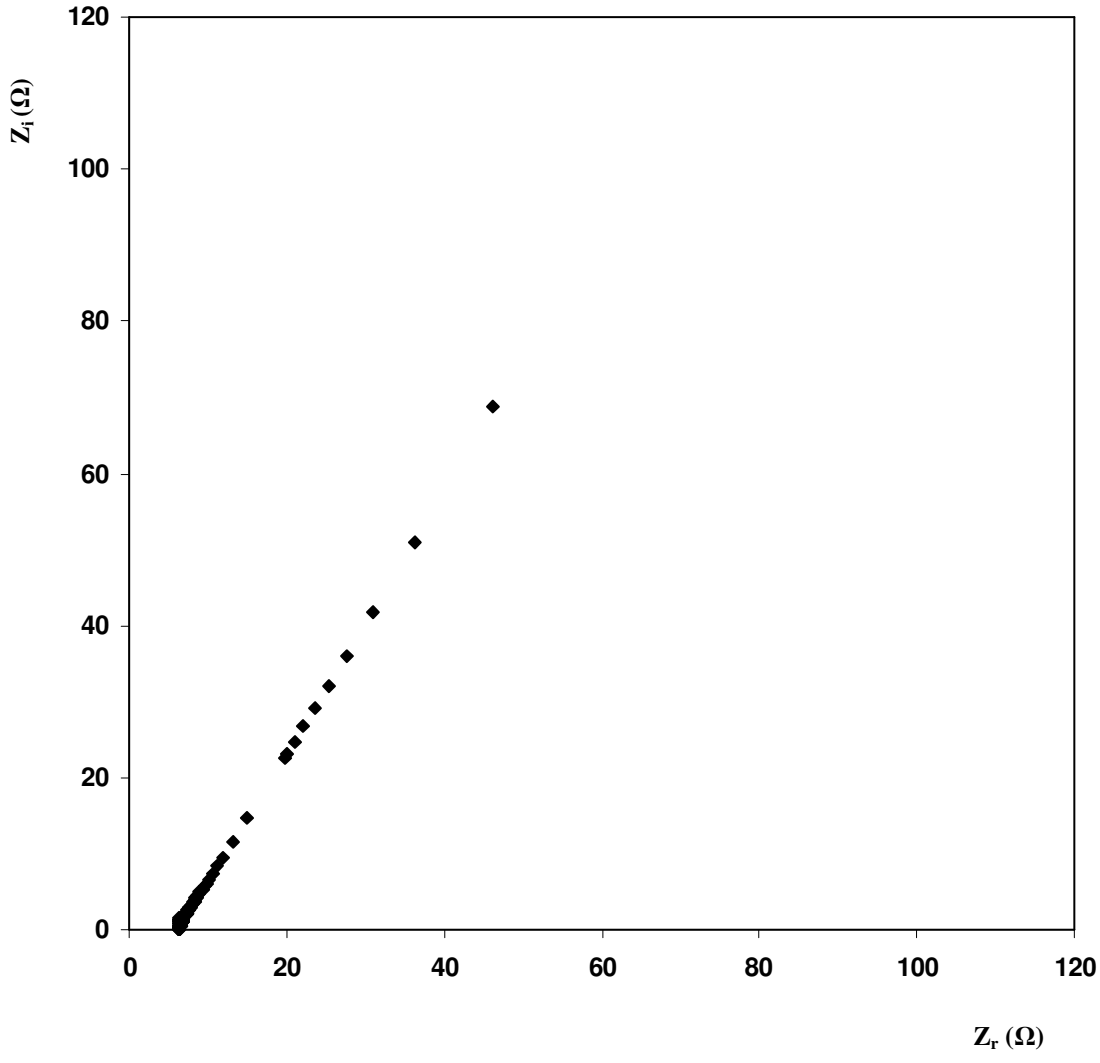

Figure 6.20: Cole-Cole plot of the sample 30[60C4P6-40AN]-70EC film.

To see the limits of dissociation of salt due to presence of EC, the highest conducting sample in the salted system (60[C4P6]-40AN sample) was studied as a function of ethylene carbonate content, Figure 6.21. It can be observed that the addition of EC has increased the conductivity in the plasticized system.

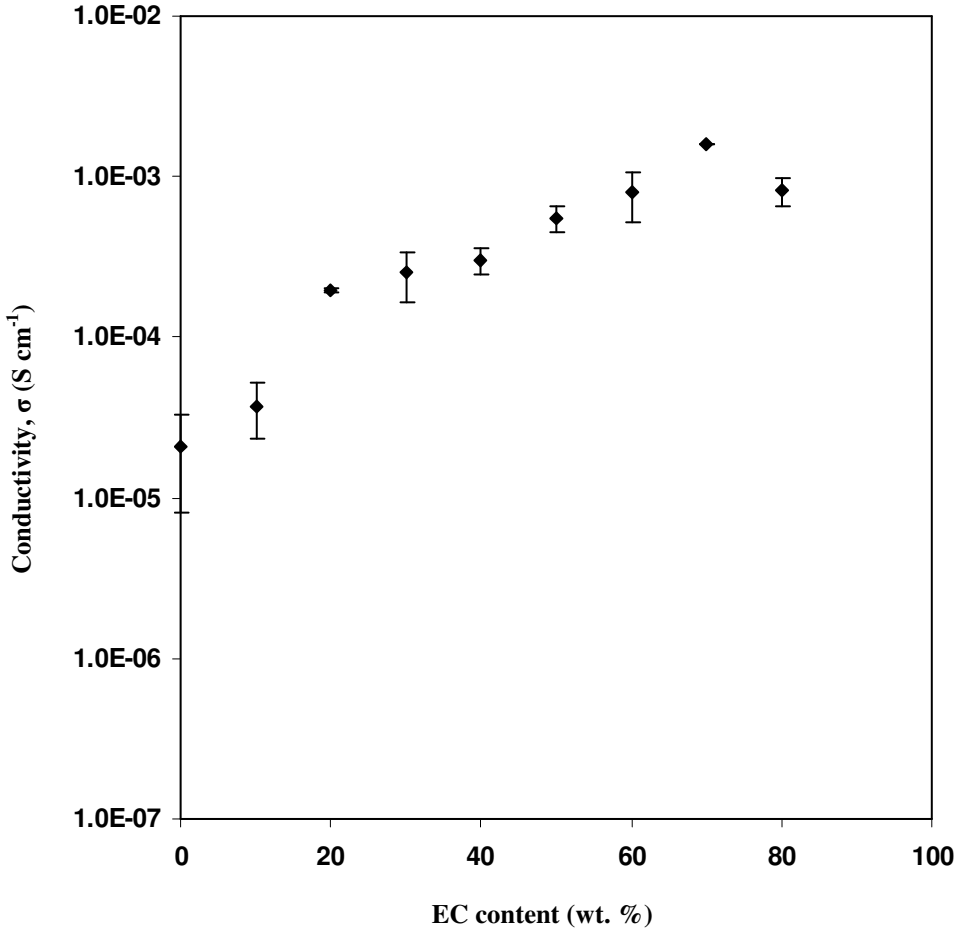

Figure 6.21: The dependence of ionic conductivity on EC at room temperature.

From Figure 6.21, the addition of EC up to 70 wt.% has increased the conductivity of PVA-chitosan-NH_4NO_3 electrolyte up to 1.60 x 10^{-3} S cm^{-1}. Addition of 80 wt.% EC concentration led to decrease in conductivity.

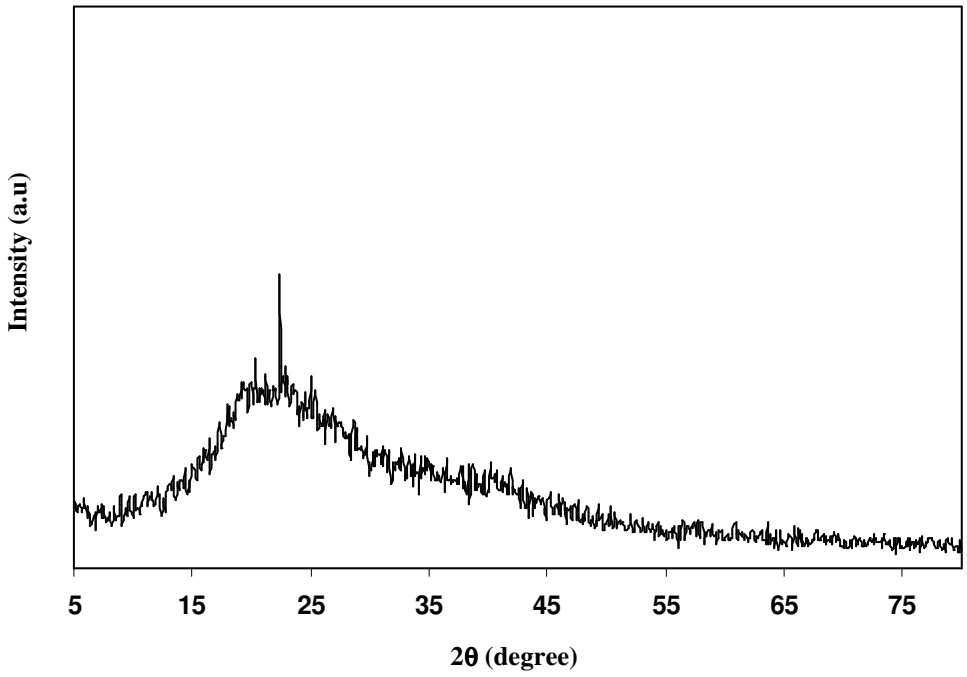

Figure 6.22: XRD diffractogram of 60[60P40C-40AN]-40EC film.

EC with high dielectric constant has been reported to increase amorphousness of polymer electrolytes. The increase in amorphousness leads to increase in conductivity [Pitawala *et al.,* 2008]. Figure 6.22 represents the X-ray diffractogram of the plasticized sample with the addition of 40 wt.% EC, sample 60[60C4P6-40AN]-40EC. The X-ray diffractogram exhibits one peak at $2\theta = 22.4°$ that could be attributed to NH_4NO_3. This implies that EC has prevented the salt from recombining to form ion aggregates that maybe trapped beneath a thin layer of polymer host. Since there are now more mobile ions in the sample, the conductivity of the plasticized sample should be higher than the 60[C4P6]-40AN electrolyte. EC also helps to dissociate NH_4NO_3 since it is known that not all of the salt dissociates into ions during preparation and during film formation.

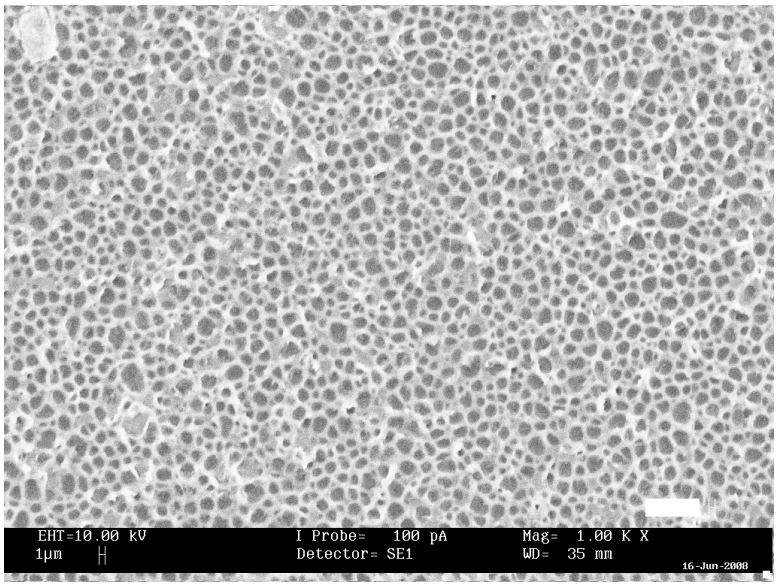

Figure 6.23: SEM images of 60[60C4P6-40AN]-40EC film.

Figure 6.23 represents the SEM surface morphology of the sample 60[60C4P6-40AN]-40EC. It can be observed that the grain-like morphology of the 60[C4P6]-40AN surface, Figure 6.5 has transformed into a honey-comb structure over a smooth morphology when 40 wt.% EC has been added to the 60[C4P6]-40AN sample.

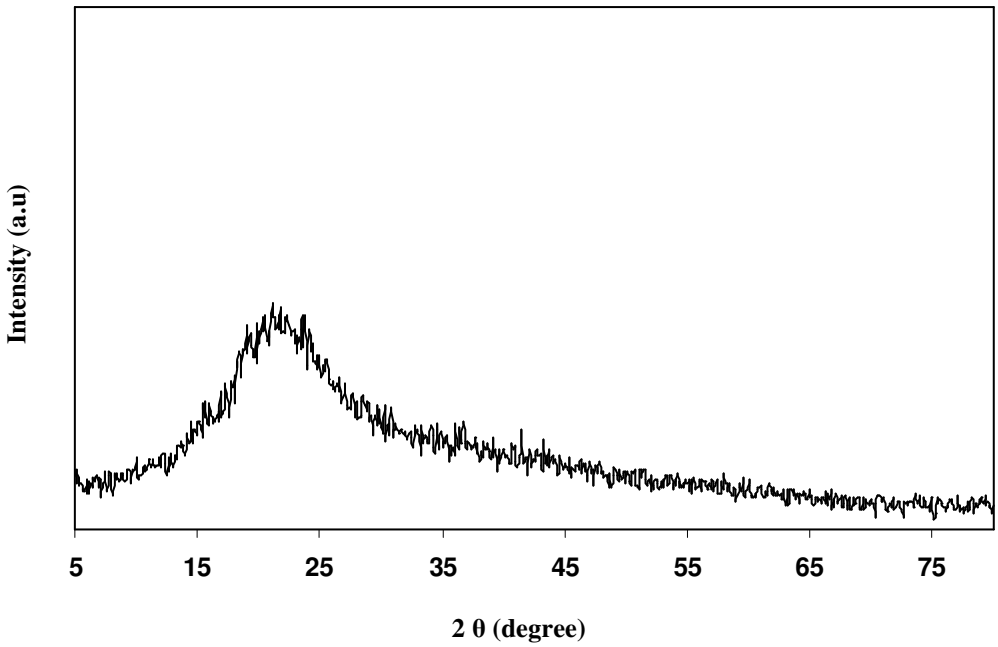

Figure 6.24: XRD diffractogram of 40[60C4P6-40AN]-60EC film.

Figure 6.24 represents the X-ray diffractogram of the plasticized sample with the addition of 60 wt. % EC, 40[60C4P6-40AN]-60EC. It is clearly seen that the sample is amorphous with no peaks appearing in the diffractogram as compared with the sample 60[60C4P6-40AN]-40EC, Figure 6.22 which means that the salt does not undergo any recrystallization process. The addition of 60 wt.% of EC has turned the sample to become more amorphous and leads towards increment in conductivity value.

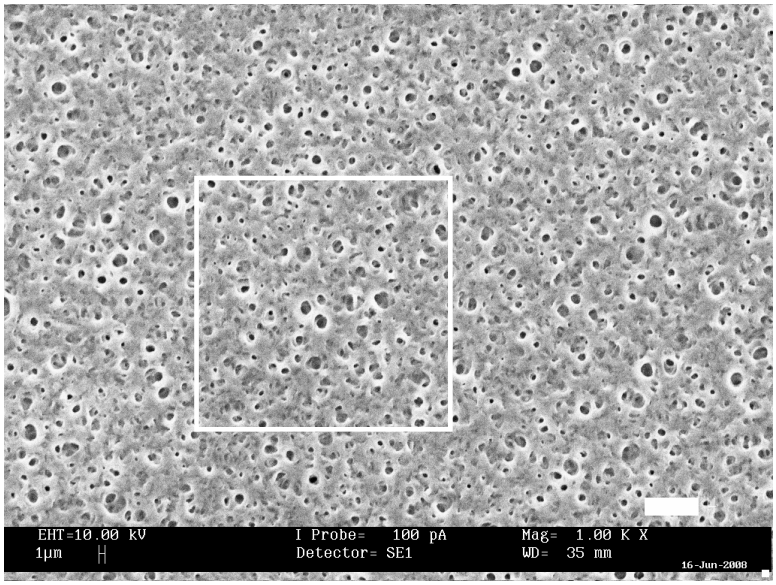

Figure 6.25: SEM images of 40[60C4P6-40AN]-60EC film.

Figure 6.25 shows the SEM surface morphology of the 40[60C4P6-40AN]-60EC sample. When 60 wt.% EC was added, the salt also does not undergo recrystallization as shown in Figure 6.24. From the SEM, it can be seen that the addition of 60 wt.% EC has turned the sample into a porous type of surface. This phase leads to the increase in diffusivity of charge carriers and contribute to conductivity enhancement. According to Xi *et al.,* (2006) the increase in porosity can increase the conductivity of the electrolytes. Figure 6.26 is the enlarged portion of 40[60C4P6-40AN]-60EC showing the pores (white circles) that can be observed on the surface of a PVA-rich sample. From scanning image probe processor, size of the pores obtain varies from 5.41 to 145.19 μm^2.

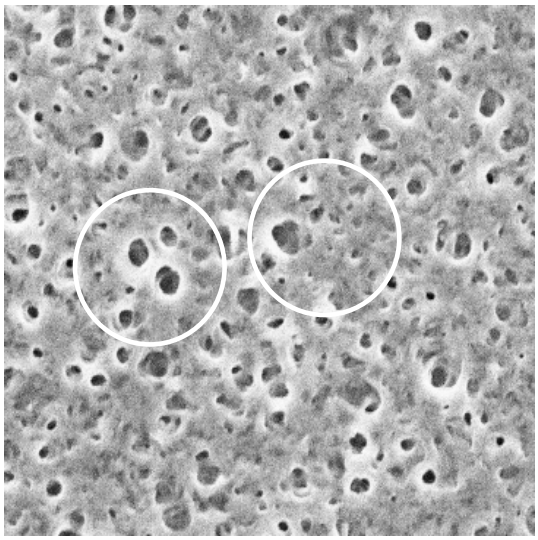

Figure 6.26: Enlarged portion of 40[60C4P6-40AN]-60EC showing the pores (white circles) that can be observed on the surface of the film

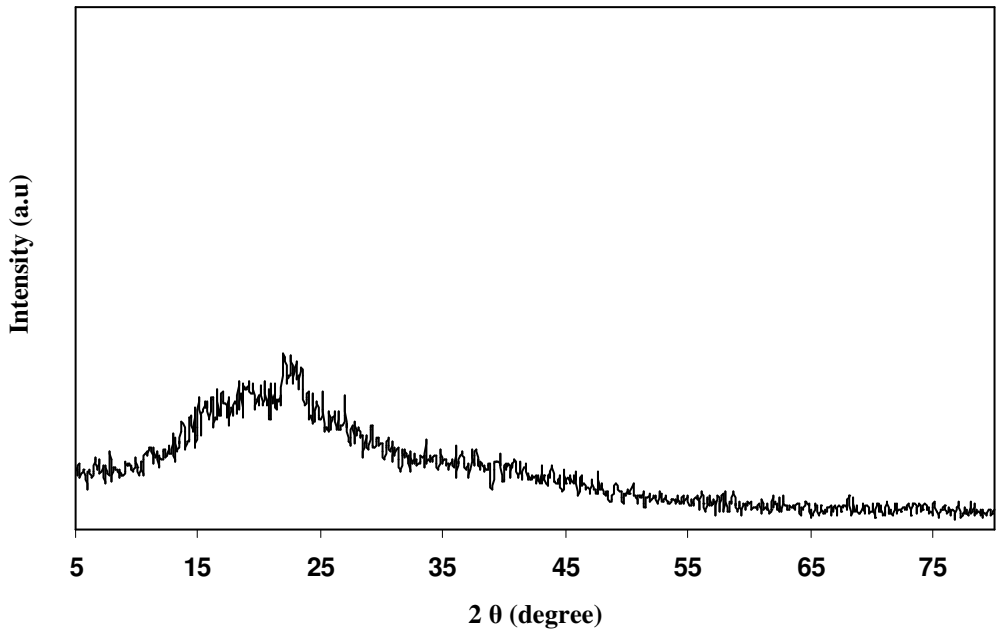

Figure 6.27: XRD diffractogram of 30[60C4P6-40AN]-70EC film

Figure 6.27 represents the X-ray diffractogram of the plasticized sample with the addition of 70 wt.% EC, 30[60C4P6-40AN]-70EC. It can be seen that the FWHM of the XRD hump in the Figure 6.27 is the longest compared to the FWHM of the XRD humps in Figures 6.22 and 6.24.

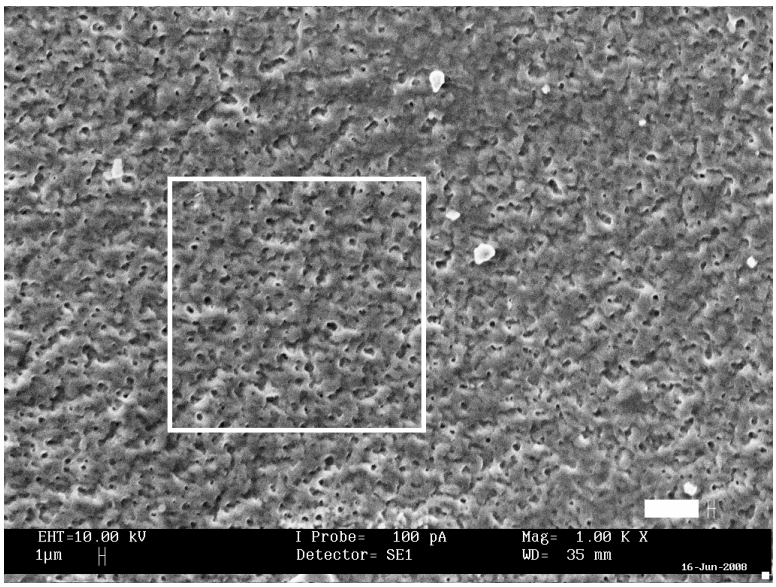

Figure 6.28: SEM images of 30[60C4P6-40AN]-70EC film.

Figure 6.28 represents the surface morphology of the 30[60C4P6-40AN]-70EC film. It can be seen that with further addition of EC up to 70 wt.%, the films surface become denser and more amorphous. The sample 30[60C4P6-40AN]-70EC was found to have the highest value of conductivity among the plasticized samples studied. In Figure 6.29, the size of pores in the film is smaller compared to 40[60C4P6-40AN]-60EC sample in Figure 6.26 and the pore size lies between 5.41 and 48.7 μm^2.

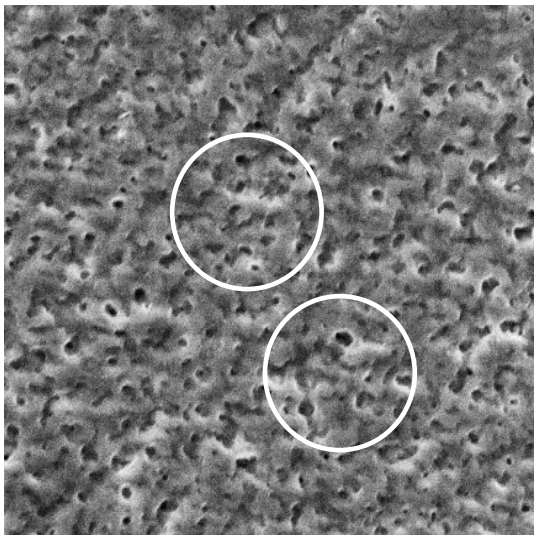

Figure 6.29: Enlarged portion of 30[60C4P6-40AN]-70EC showing the pores (white circles) that can be observed on the surface of the film.

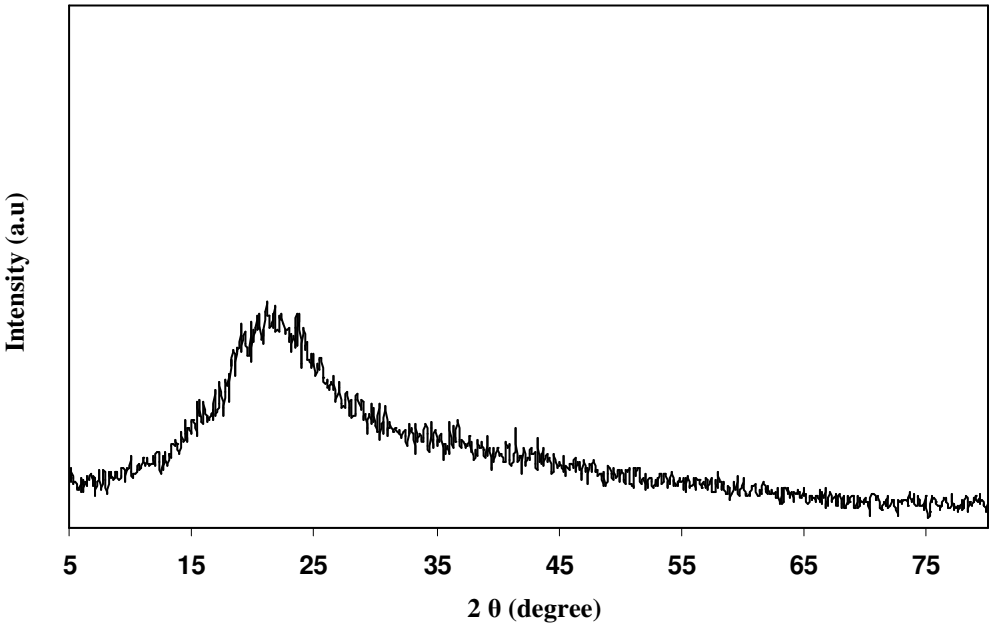

Figure 6.30: XRD diffractogram of 20[60C4P6-40AN]-80EC film.

Figure 6.30 represents the X-ray diffractogram of the plasticized sample with the addition of 80 wt.% EC, 20[60C4P6-40AN]-80EC. It can be observed that the FWHM of the XRD hump has decreased indicating that the sample has become less amorphous and more crystalline. This may explain why the conductivity of the sample is lower than for the sample with 70 wt.% EC.

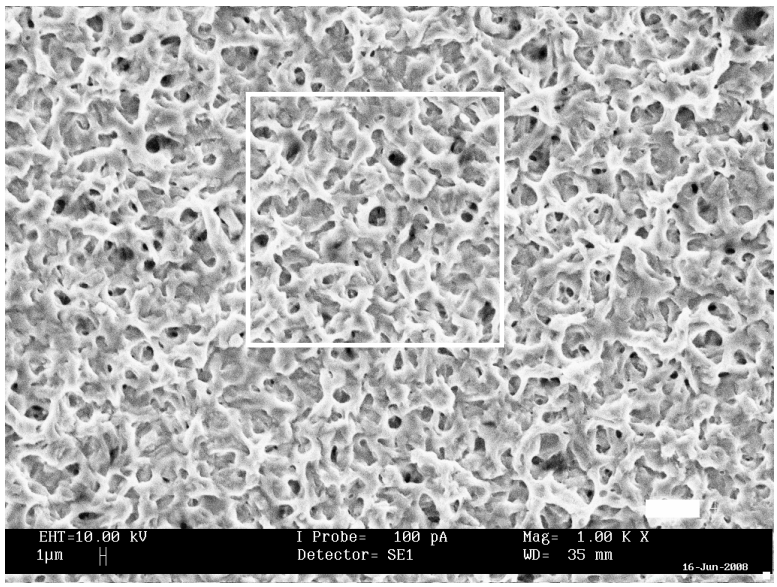

Figure 6.31: SEM images of 20[60C4P6-40AN]-80EC film.

Figure 6.31 represents the surface morphology of the film 60[60C4P6-40AN]-80EC. With addition of EC up to 80 wt.%, it has been observed that bigger pores can be seen in the sample surface. From enlarged portion of 20[60C4P6-40AN]-80EC in Figure 6.32 showing the pores with bigger size of 145 to 389.18 μm^2.

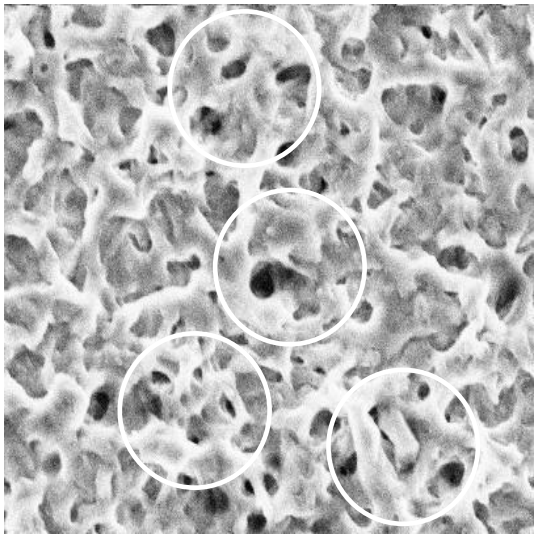

Figure 6.32: Enlarged portion of 20[60C4P6-40AN]-80EC showing the pores (white circles) that can be observed on the surface of the film.

Table 6.6: The average ionic conductivity for salted system at room temperature.

Sample designation	σ (S cm^{-1})
90[60C4P6-40AN]-10EC	2.67×10^{-5}
80[60C4P6-40AN]-20EC	1.94×10^{-4}
70[60C4P6-40AN]-30EC	2.50×10^{-4}
60[60C4P6-40AN]-40EC	2.99×10^{-4}
50[60C4P6-40AN]-50EC	5.55×10^{-4}
40[60C4P6-40AN]-60EC	7.90×10^{-4}
30[60C4P6-40AN]-70EC	1.60×10^{-3}
20[60C4P6-40AN]-80EC	8.25×10^{-4}

6.7 Dielectric Constant for Plasticized System at Room Temperature

The plots of dielectric constant for the plasticized system with different EC concentration at room temperature are as depicted in Figure 6.33. From the plot of dielectric constant in the plasticized system at room temperature, it can be observed that the values are higher as compared to the salted system. EC (donor number = 16.4) [Kim *et al.,* 2000] have a relatively low viscosity. Hence, the incorporation of EC can decrease local viscosity around the charge-transporting ions and increase ionic mobility.

EC also have a high dielectric constant (89.78) [Xu, 2004]. Hence EC is able to weaken the cation-anion attractive force and results in salt dissociation [Wintersgill, 1987]. Hence more undissociated salt become ions which increase the number of free ions that will increase the dielectric constant of the sample.

Table 6.6 shows that σ (30[60C4P6-40AN]-70EC) > σ (20[60C4P6-40AN]-80EC) > σ (40[60C4P6-40AN]-60EC) > σ (50[60C4P6-40AN]-50EC) > σ (60[60C4P6-40AN]-40EC) > σ (70[60C4P6-40AN]-30EC) > σ (80[60C4P6-40AN]-20EC) > σ (90[60C4P6-40AN]-10EC) and the dielectric constant also increases follows the same trend ε_r (30[60C4P6-40AN]-70EC) > ε_r (20[60C4P6-40AN]-80EC) > ε_r (40[60C4P6-40AN]-60EC) > ε_r (50[60C4P6-40AN]-50EC) > ε_r (60[60C4P6-40AN]-40EC) > ε_r (70[60C4P6-40AN]-30EC) > ε_r (80[60C4P6-40AN]-20EC) > ε_r (90[60C4P6-40AN]-10EC).

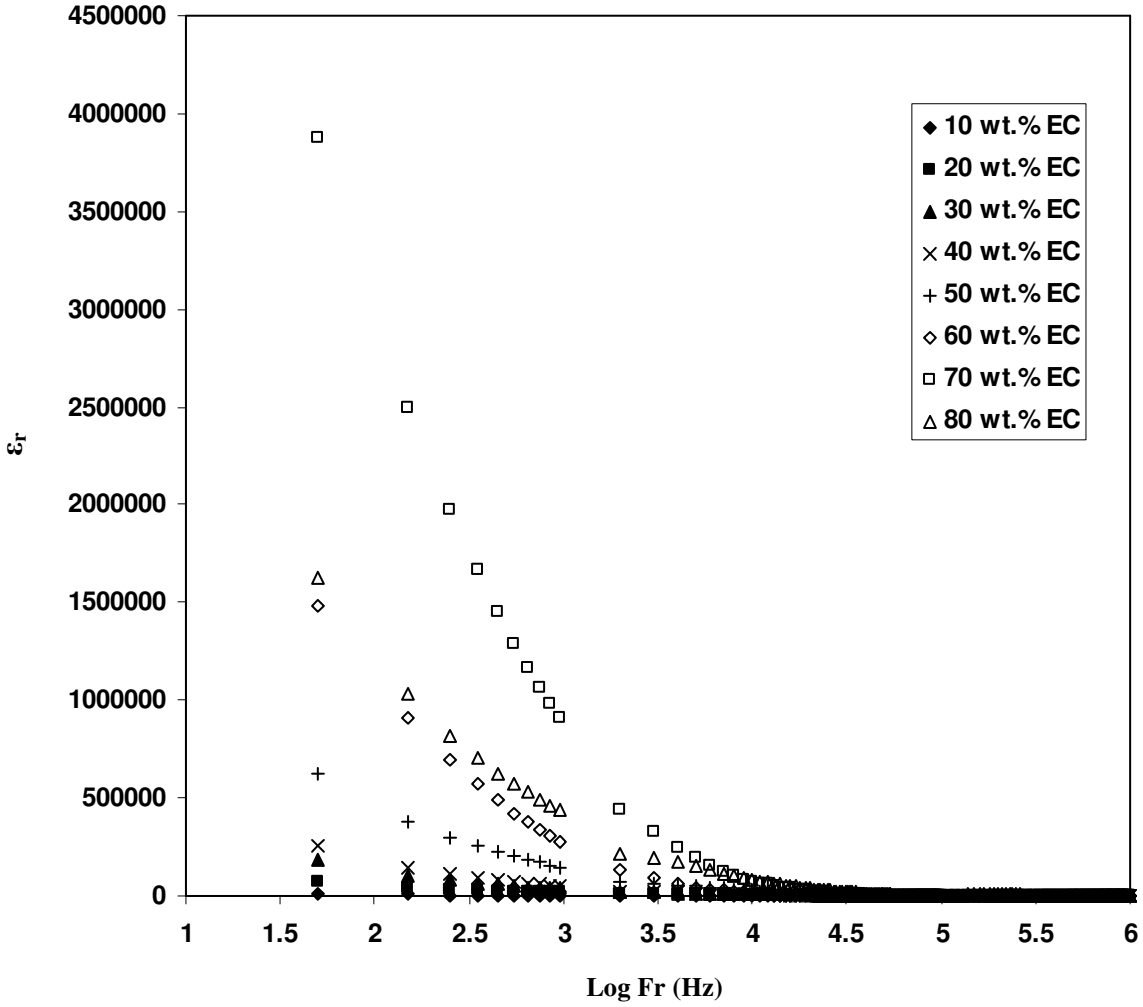

Figure 6.33: Dielectric constant versus frequency for plasticized system with different EC concentration at room temperature.

6.7.1 Dielectric Constant of Film Sample 30[60C4P6-40AN]-70EC at Elevated Temperatures

The variation of the dielectric constant for the highest conducting sample in the plasticized system with the concentration of 70 wt. % EC (30[60C4P6-40AN]-70EC) as a function of frequency at elevated temperatures is depicted in Figure 6.34. At higher temperatures, the dielectric constant has been observed to have a higher value which is attributable to the higher charge carrier density. This indicates that as temperature

increases, the degree of salt dissociation increases which causes the increase in the number of free ions and in turn increase the conductivity of the sample.

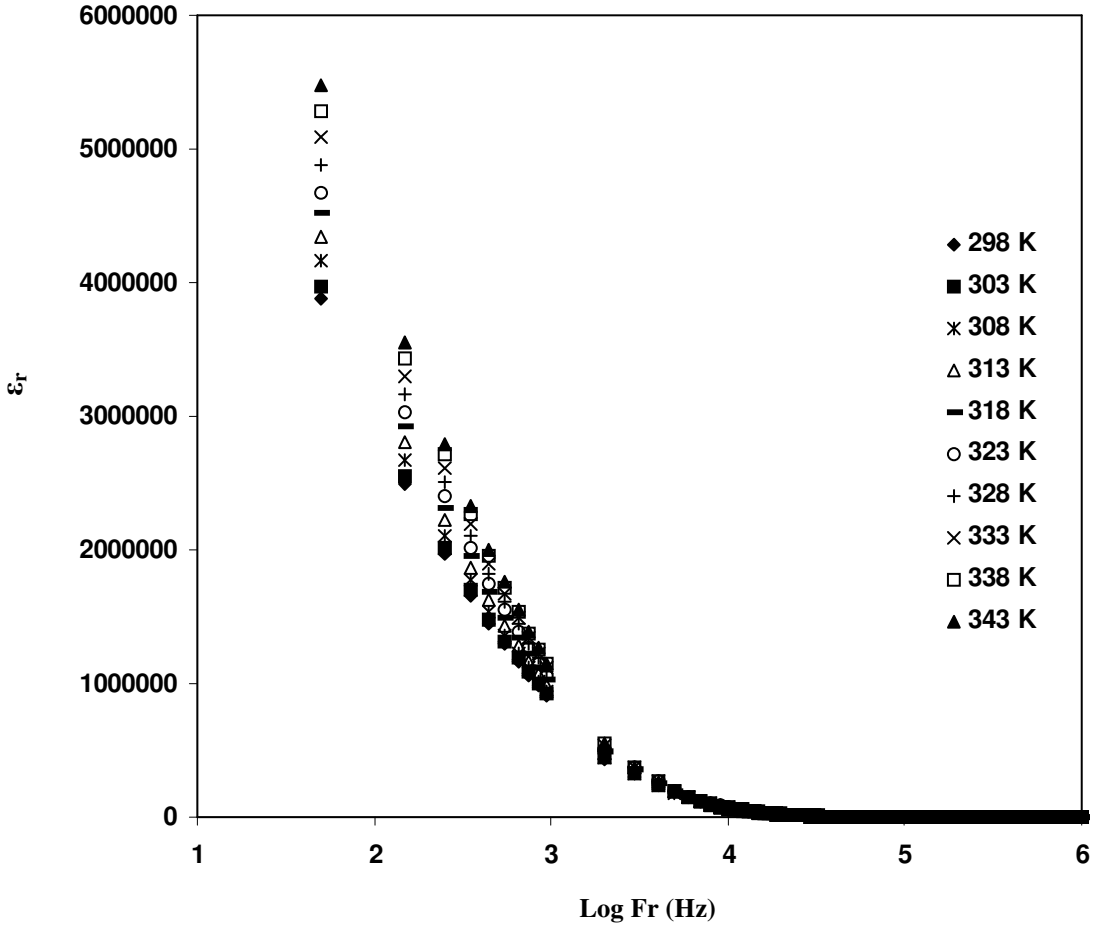

Figure 6.34: Dielectric constant versus frequency for 30[60C4P6-40AN]-70EC sample at different temperature.

6.8 Temperature Dependence of Conductivity (Plasticized System)

Figure 6.35 represents the conductivity of the plasticized system with different concentrations of plasticizer, EC at elevated temperatures. The figure shows that as temperature increases, the conductivity increases.

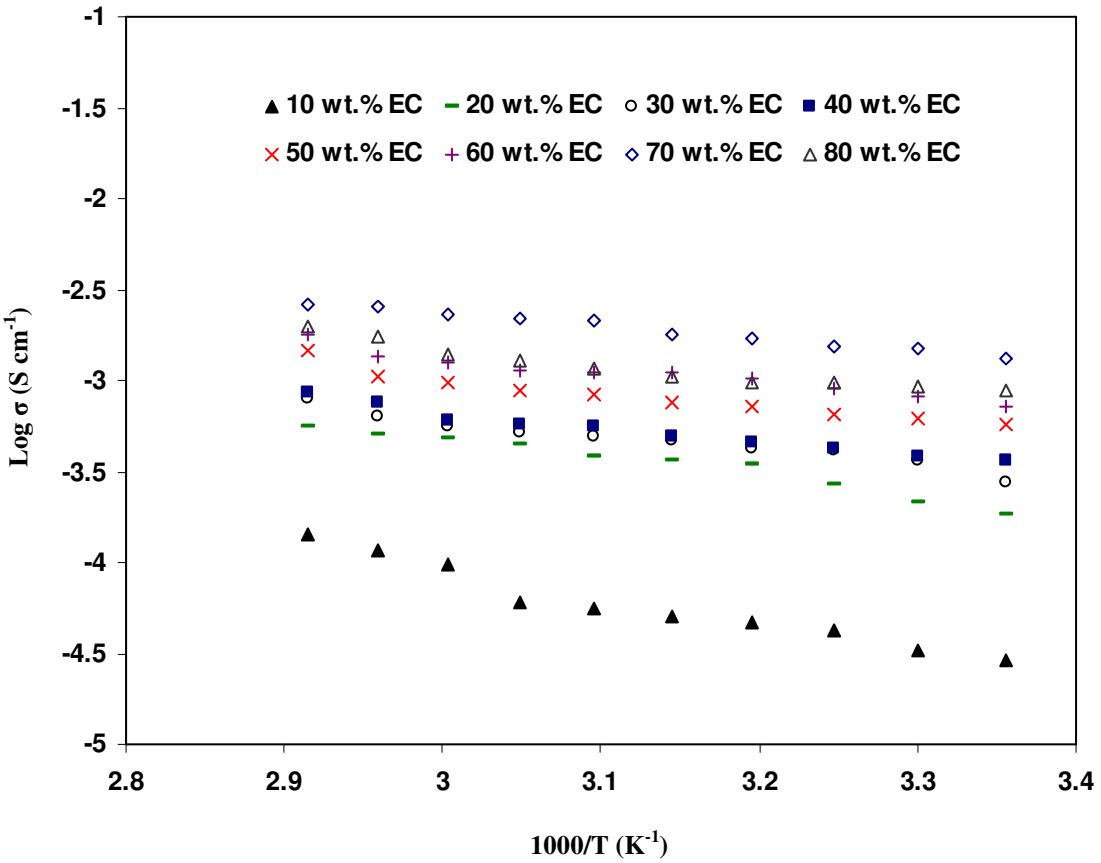

Figure 6.35: Temperature dependent conductivity for plasticized system with different plasticizer concentration.

Regression (R^2) values for all samples are close to unity indicating that all points tend to lie on a straight line. It can be observed that the behavior of the conductivity is thermally assisted. For the plasticized system at 70 wt.% EC temperature dependent conductivity is comparable with Ng and Mohamad, (2008). They suggested that the temperature dependent conductivity in their work follows Arrhenius behavior.

Figure 6.36 represents the activation energy and the conductivity plot of plasticized system.

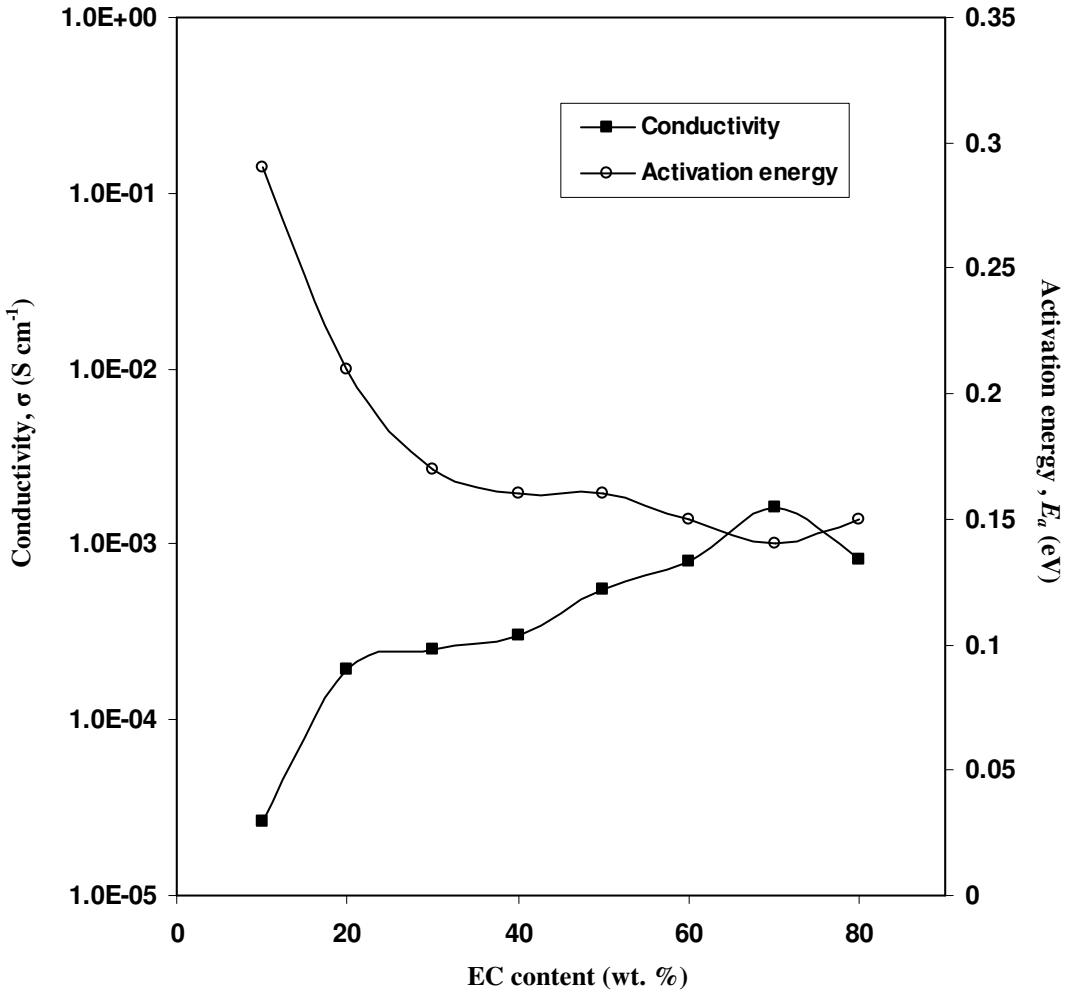

Figure 6.36: Activation energy for plasticized system.

It is observed that the 30[60C4P6-40AN]-70EC sample (the highest conducting sample) has the lowest activation energy where the value is 0.14 eV. This result is comparable with Ng and Mohamad, (2008) where the value of the activation energy is ~ 0.1 eV with conductivity value of ~ 10^{-3} S cm^{-1}. The regression value and the activation energy of plasticized system are tabulated in Table 6.7. These results are expected from the conduction mechanism scheme proposed in Figure 5.22.

Table 6.7: Regression, R^2 and activation energy, E_a value for plasticized system.

Sample	R^2	E_a (eV)
90[60C4P6-40AN]-10EC	0.94	0.29
80[60C4P6-40AN]-20EC	0.97	0.21
70[60C4P6-40AN]-30EC	0.96	0.17
60[60C4P6-40AN]-40EC	0.94	0.16
50[60C4P6-40AN]-50EC	0.92	0.16
40[60C4P6-40AN]-60EC	0.93	0.15
30[60C4P6-40AN]-70EC	0.99	0.14
20[60C4P6-40AN]-80EC	0.91	0.15

6.9 The Rice and Roth Model for Plasticized System

It can be seen from Table 6.8 that the incorporation of EC into the polymer-salt system has produced more mobile ions and has also lowered the viscosity of the salted electrolyte that led to the increase in ionic mobility. The addition of EC which has a high dielectric constant promotes the dissociation of NH_4NO_3 into free ions leading to an increase in the charge carriers as shown in Table 6.6**.** From Tables 6.9 and 6.10, it can be observed that when the *l* value changes, the number density and mobility of mobile ions still follow the trend of conductivity in the plasticized system and the values are higher as compared to the value in the salted system for l = 6 and 3 Å respectively.

Table 6.8: Transport parameters for plasticized system at room temperature (using l = 10 Å).

Sample	τ (s)	n (cm^{-3})	μ ($cm^2 V^{-1} s^{-1}$)
90[60C4P6-40AN]-10EC	1.34×10^{-13}	7.98×10^{19}	2.09×10^{-6}
80[60C4P6-40AN]-20EC	1.57×10^{-13}	3.72×10^{20}	3.27×10^{-6}
70[60C4P6-40AN]-30EC	1.75×10^{-13}	3.92×10^{20}	3.98×10^{-6}
60[60C4P6-40AN]-40EC	1.80×10^{-13}	4.48×10^{20}	4.17×10^{-6}
50[60C4P6-40AN]-50EC	1.80×10^{-13}	8.32×10^{20}	4.17×10^{-6}
40[60C4P6-40AN]-60EC	1.86×10^{-13}	1.13×10^{21}	4.36×10^{-6}
30[60C4P6-40AN]-70EC	1.93×10^{-13}	2.20×10^{21}	4.54×10^{-6}
20[60C4P6-40AN]-80EC	1.86×10^{-13}	1.18×10^{21}	4.36×10^{-6}

Table 6.9: Transport parameters for plasticized system at room temperature (using l = 6 Å).

Sample	τ (s)	n (cm^{-3})	μ ($cm^2 V^{-1} s^{-1}$)
90[60C4P6-40AN]-10EC	8.03×10^{-14}	1.33×10^{20}	1.25×10^{-6}
80[60C4P6-40AN]-20EC	9.43×10^{-14}	6.19×10^{20}	1.96×10^{-6}
70[60C4P6-40AN]-30EC	1.05×10^{-13}	6.54×10^{20}	2.39×10^{-6}
60[60C4P6-40AN]-40EC	1.08×10^{-13}	7.46×10^{20}	2.50×10^{-6}
50[60C4P6-40AN]-50EC	1.08×10^{-13}	1.39×10^{21}	2.50×10^{-6}
40[60C4P6-40AN]-60EC	1.12×10^{-13}	1.89×10^{21}	2.61×10^{-6}
30[60C4P6-40AN]-70EC	1.16×10^{-13}	3.66×10^{21}	2.72×10^{-6}
20[60C4P6-40AN]-80EC	1.12×10^{-13}	1.97×10^{21}	2.61×10^{-6}

Table 6.10: Transport parameters for plasticized system at room temperature (using l = 3 Å).

Sample	τ (s)	n (cm^{-3})	μ ($cm^2 V^{-1} s^{-1}$)
90[60C4P6-40AN]-10EC	4.01×10^{-14}	2.66×10^{20}	6.27×10^{-7}
80[60C4P6-40AN]-20EC	4.72×10^{-14}	1.24×10^{21}	9.80×10^{-7}
70[60C4P6-40AN]-30EC	5.24×10^{-14}	1.31×10^{21}	1.19×10^{-6}
60[60C4P6-40AN]-40EC	5.40×10^{-14}	1.49×10^{21}	1.25×10^{-6}
50[60C4P6-40AN]-50EC	5.40×10^{-14}	2.77×10^{21}	1.25×10^{-6}
40[60C4P6-40AN]-60EC	5.58×10^{-14}	3.78×10^{21}	1.31×10^{-6}
30[60C4P6-40AN]-70EC	5.78×10^{-14}	7.33×10^{21}	1.36×10^{-6}
20[60C4P6-40AN]-80EC	5.58×10^{-14}	3.95×10^{21}	1.31×10^{-6}

Figures 6.37 and 6.38 represents the variation of number density of mobile ions, n and mobility, μ of ions as functions of temperature respectively using l = 10 Å. It is clearly observed that the number density of mobile ions increases as the temperature increases as depicted in Figure 6.37. The mobility of ions also increases as the temperature increases however the increment is not so obvious as compared to the number density of ions. Hence, it can be concluded that the conductivity is controlled by the number of mobile ions (charge carriers) in all films. Figures 6.39 and 6.40 represents the number density of mobile ions, n and mobility μ as a function of temperature using l = 6 Å. It can be observed that the trend at various temperature follows the same trend using l = 10 Å. The same trend also can be observed when l = 3 Å applied and is depicted in Figures 6.41 and 6.42.

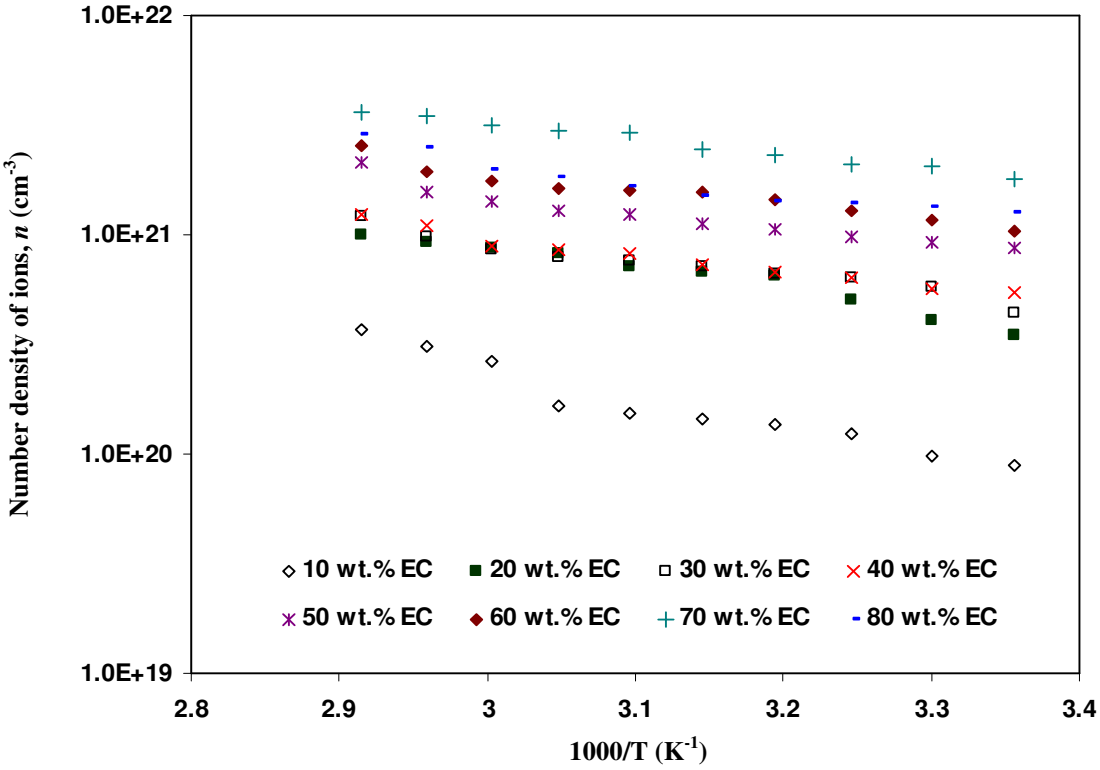

Figure 6.37: Number density of mobile ions, *n* as a function of temperature for plasticized system for *l* = 10 Å.

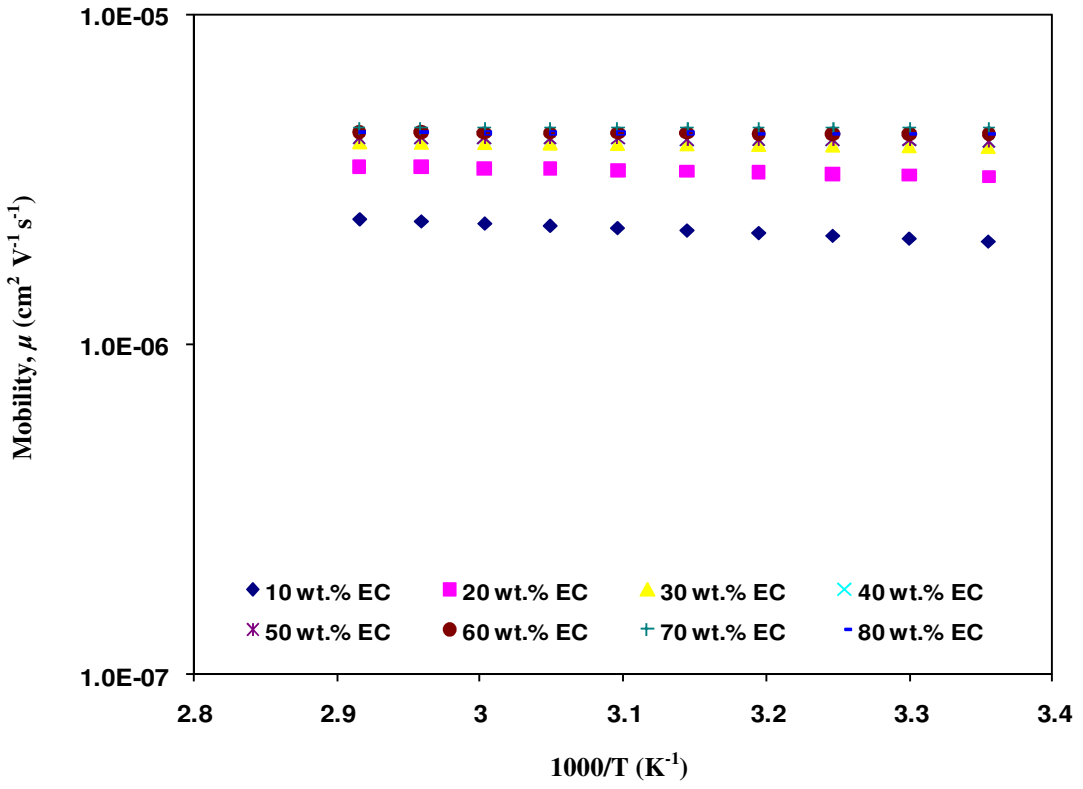

Figure 6.38: Ionic mobility of ions, *μ* as a function of temperature for plasticized system for *l* = 10 Å.

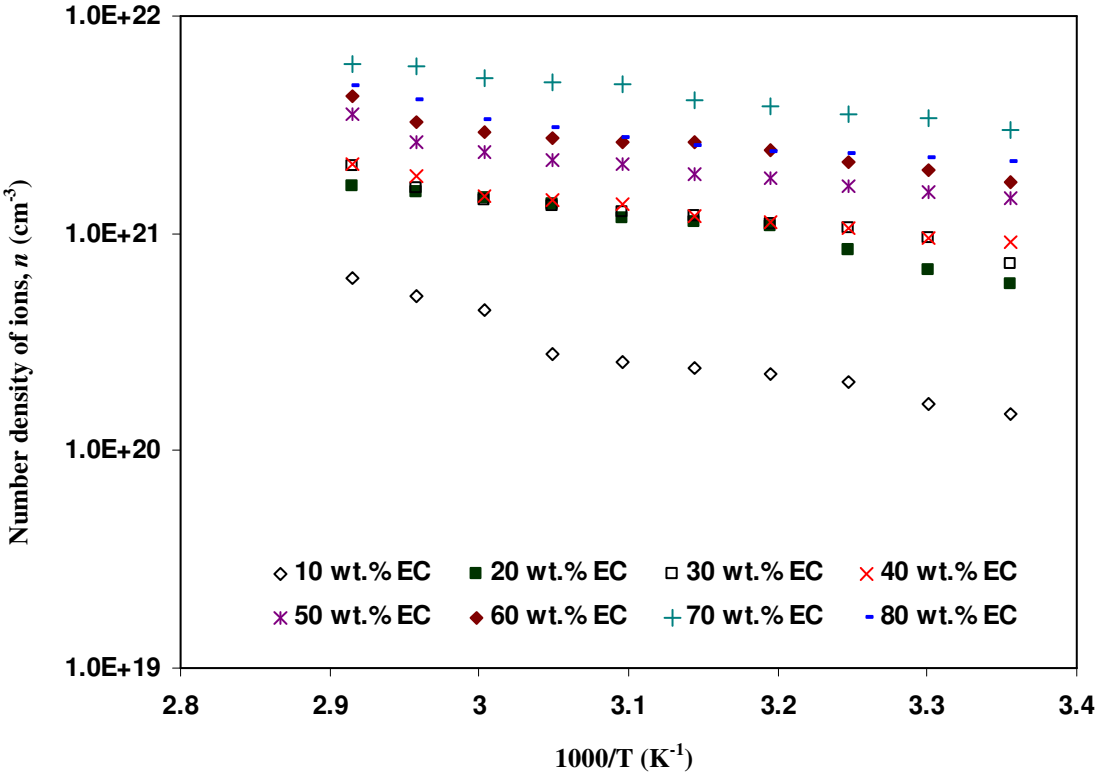

Figure 6.39: Number density of mobile ions, n as a function of temperature for plasticized system for l = 6 Å.

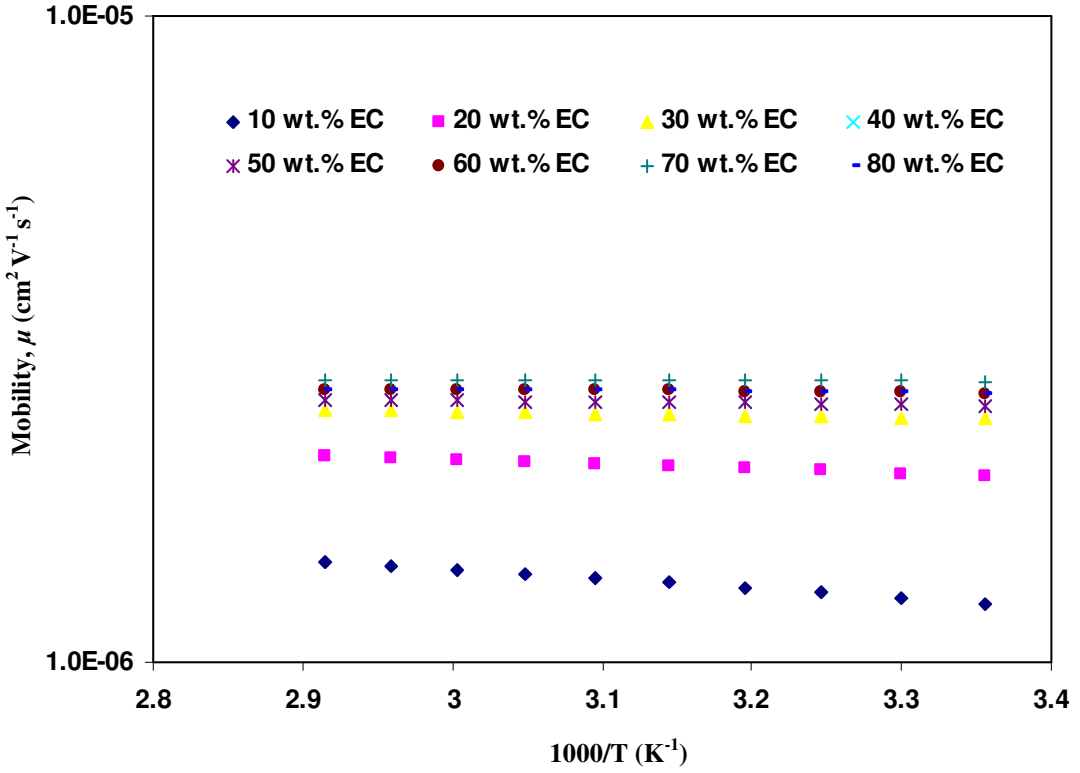

Figure 6.40: Ionic mobility of ions, μ as a function of temperature for plasticized system for l = 6 Å.

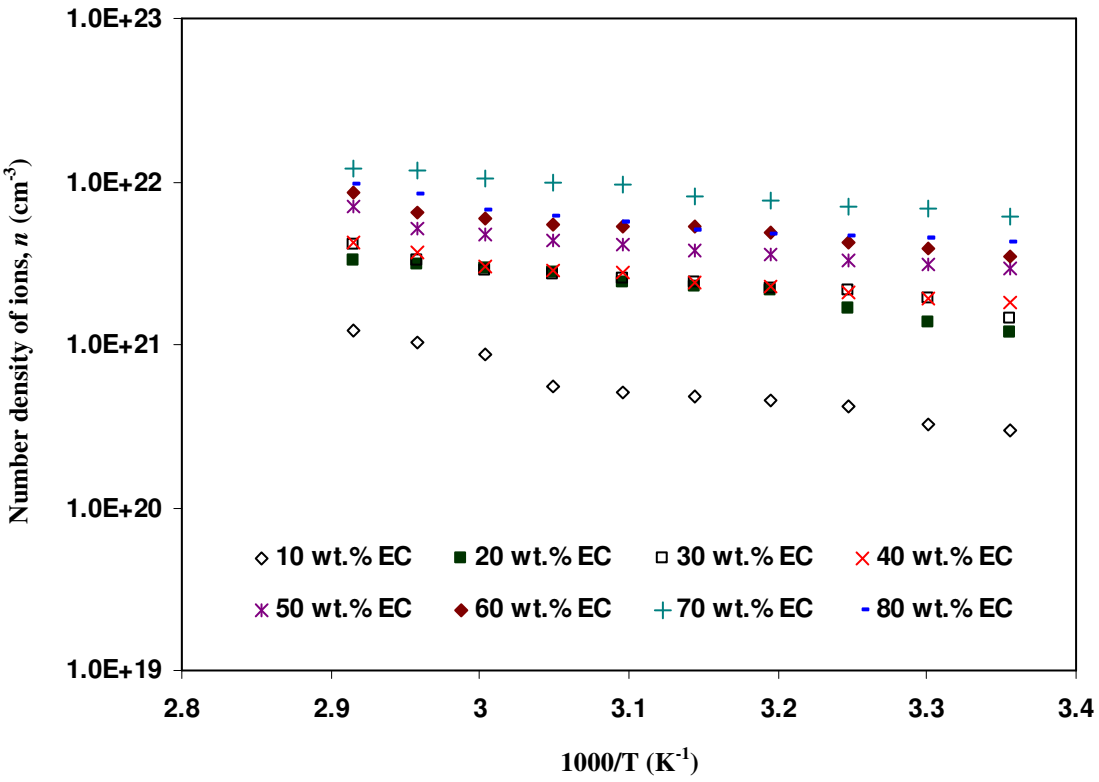

Figure 6.41: Number density of mobile ions, *n* as a function of temperature for plasticized system for *l* = 3 Å.

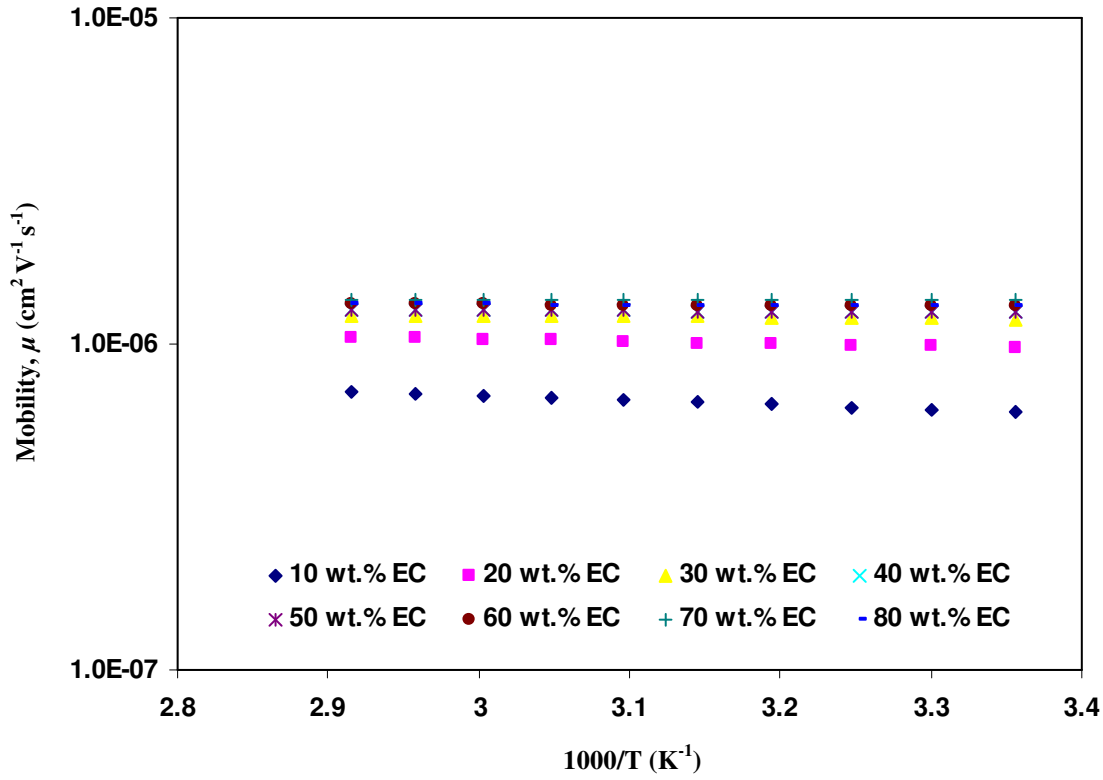

Figure 6.42: Ionic mobility of ions, *μ* as a function of temperature for plasticized system for *l* = 3 Å.

6.10 Summary

The electrical conductivity of PVA-chitosan blend based polymer electrolytes have been presented. The highest conductivity for the salted system at room temperature was obtained to be 2.07 x 10^{-5} S cm^{-1} at 40 wt.% NH_4NO_3 concentration (sample 60[C4P6]-40AN). Addition of EC has increased the conductivity value of the highest conducting sample in salted system. The plasticized sample at room temperature with 70 wt.% EC concentration was found to have a maximum value at 1.60 x 10^{-3} S cm^{-1} (sample 30[60C4P6-40AN]-70EC).

Conductivity studies at elevated temperatures for both salted and plasticized systems in this work imply that the conductivity is thermally assisted and the calculation of activation energy inferred that the highest conducting sample possessed the lowest activation energy and vice versa.

The dielectric constant, ε_r studies were observed to follow the trend of the conductivity studies for all systems. At different temperatures, the dielectric constants of both systems are also in accordance with the conductivity value. The sample with the highest conductivity value possessed the highest value of dielectric constant.

Transport parameters for both salted and plasticized system has been calculated employing the Rice and Roth model. The conductivity values in both systems are controlled by the number density of mobile ions.